DCG

GJBX-2(84)

National Uranium Resource Evaluation

PARAMETER ASSIGNMENTS FOR SPECTRAL GAMMA-RAY BOREHOLE CALIBRATION MODELS

Bendix Field Engineering Corporation
Grand Junction, Colorado

April 1984

PREPARED FOR THE U.S. DEPARTMENT OF ENERGY
Assistant Secretary for Nuclear Energy
Grand Junction Area Office, Colorado

This report is a result of work performed by Bendix Field Engineering Corporation, Operating Contractor for the U.S. Department of Energy, as part of the National Uranium Resource Evaluation. NURE was a program of the U.S. Department of Energy's Grand Junction, Colorado, Office to acquire and compile geologic and other information with which to assess the magnitude and distribution of uranium resources and to determine areas favorable for the occurrence of uranium in the United States.

Available from: Technical Library
Bendix Field Engineering Corporation
P.O. Box 1569
Grand Junction, CO 81502–1569

Telephone: (303) 242–8621, Ext. 278

Price per Microfiche Copy: $4.50

GJBX-2(84)

PARAMETER ASSIGNMENTS FOR SPECTRAL GAMMA-RAY BOREHOLE CALIBRATION MODELS

B. E. Heistand and E. F. Novak
Bendix Field Engineering Corporation
Grand Junction Operations
Grand Junction, Colorado

April 1984

Prepared for the U.S. Department of Energy
Assistant Secretary for Nuclear Energy
Grand Junction Area Office
Grand Junction, Colorado
Under Contract No. DE-AC07-76GJ01664

CONTENTS

APPENDICES

(microfiche in pocket, back inside cover)

ILLUSTRATIONS

TABLES

ABSTRACT

This report documents the work performed to determine the newly assigned concentrations for the spectral gamma-ray borehole calibration models. Thirty-two models, maintained by the U.S. Department of Energy, are included in this study, and are grouped into eight sets of four models each. The eight sets are located at sites across the United States, and are used to calibrate logging instruments. The assignments are based on in-situ logging data to ensure self-consistency in the assigned concentrations, and on laboratory assays of concrete samples from each model to provide traceability to the New Brunswick Laboratory (NBL) standards.

1.0 INTRODUCTION

This report presents the results of work performed to determine radioelement concentrations for the spectral gamma-ray borehole calibration models that are used to calibrate logging instruments. These concentrations are based on in-situ logging data to ensure self-consistency, and on laboratory assays of concrete samples from each model to provide traceability to the New Brunswick Laboratory (NBL) standards. A self-consistent assignment implies that the calibration coefficients determined in any one set of calibration models are equivalent to those determined in any other set. Requiring traceability to the NBL standards implies that the concentrations assigned to the models are in agreement with the national standards used for laboratory assays. The standards used for this study are the NBL 100A Series for uranium and thorium, and reagent-grade potassium carbonate (K_2CO_3) for potassium. Laboratory assays were performed by the Bendix Field Engineering Corporation (Bendix) Geochemistry Laboratory; Bendix is the operating contractor for the Department of Energy (DOE) Grand Junction, Colorado, Area Office.

1.1 CALIBRATION MODELS

The Department of Energy maintains several models at sites across the United States for use in calibrating radiometric assay instruments. The models discussed in this report are used to calibrate borehole instruments that are used to measure in-situ concentrations of potassium, uranium, and thorium (KUT) by measuring the gamma-ray activities of these radioactive elements in the borehole environment. Each of the models has a central zone in which the concrete mix is enriched with an indicated radioactive element(s) in the form of various ores and sands. This central zone is 4 to 5 feet thick depending on the model, and lies between an upper and a lower barren zone, neither of which contains any radioactive enrichment.

The thirty-two models used for calibrating KUT assay probes are arranged in eight sets of four models each. This is a functional arrangement, in that calibration of an instrument typically involves measurements taken in only one of the eight sets of models. The eight sets are located as follows: two sets in Grand Junction, Colorado; and one set each in Casper, Wyoming; Spokane, Washington; Reno, Nevada; Morgantown, West Virginia; George West, Texas; and Grants, New Mexico.

Of the two sets of models at Grand Junction, one is the original set used for KUT calibration work. This original set initially consisted of three models known as the K, U, and T models, named for the radioelement used to enrich the central zone of concrete. A fourth model, later added to these three, is called the KUT water factor (KW) model, and its central zone is enriched with all three radioactive elements.

The other seven sets of models, known as the B models, were created more recently. Each set of these B models also contains four models: BK (potassium), BU (uranium), BT (thorium), and BM (mixed radioelements). To identify a specific model, each site has an identifying letter, which is used as part of the model's designation (i.e., CBU identifies the uranium-enriched B model at Casper, Wyoming). Table 1-1 lists the location and designation of each model included in this study.

Table 1-1. Location and Designation of the Calibration Models

Location	Model Designation
Grand Junction, Colorado	K,U,T,KW,BK,BU,BT,BM
Casper, Wyoming	CBK,CBU,CBT,CBM
George West, Texas	TBK,TBU,TBT,TBM
Grants, New Mexico	GBK,GBU,GBT,GBM
Morgantown, West Virginia	MBK,MBU,MBT,MBM
Reno, Nevada	RBK,RBU,RBT,RBM
Spokane, Washington	SBK,SBU,SBT,SBM.

1.2 RATIONALE FOR CURRENT CONCENTRATION ASSIGNMENTS

This concentration-assignment work represents the first effort to assign KUT concentrations to the B models. The prior lack of official assignments made it impossible to use the large majority of available models as standards for calibration purposes.

Concentrations for the original set of calibration models (K, U, T, and KW) have also been redetermined because the method of assigning concentrations used in this study differs from the method used in the past. In the past, the concentrations assigned to the KUT calibration models were simply the averages of the assay values determined by the Geochemistry Laboratory for the concrete samples taken from the models (Knapp and Bush, 1976). A potential problem with this earlier method of parameter assignment is the fact that sampling errors may be overlooked (George and others, 1983). Sampling problems occur when the average concentration of the concrete samples assayed by the laboratory is not equal to the average concentration of the model as seen from the borehole as a result of either inhomogeneities in the concrete-ore mixture or problems associated with the sample preparation technique. This discrepancy between the laboratory assay concentration and the in-situ concentration at the borehole creates a problem with respect to the self-consistency of the models. Steps were taken in this study to minimize the effects of sampling error.

1.3 BRIEF DESCRIPTION OF METHOD

The method used in this study to establish concentrations for the spectral gamma-ray borehole calibration models minimizes the effects of potential sampling error as described above, yet maintains the same traceability to the NBL standards. Two sets of data were acquired: laboratory assay values with traceability to the NBL standards and in-situ logging measurements taken with a high-purity germanium (HPGe) detector system. The count-rate data from the HPGe detector have a high degree of self-consistency, subject only to the constraints imposed by Poisson counting statistics on the repeatability of the measurements.

Theory concerning gamma-ray production, transport, and detection predicts that the photopeak count rates measured in the borehole are related to the concen-

trations of the associated radioactive elements (Wilson, 1981). Corrections were applied to the observed data to make this relationship linear.

Three correction factors were applied to the count-rate data. The first corrected for the dead time of the detector system. The second corrected for the presence of moisture in the model. The third factor corrected the potassium-peak (1461-keV) count rate for contributions from an actinium peak (1459 keV), which is a thorium daughter.

A single correction was made to the laboratory assay concentrations. This correction was made to the reported uranium concentration to correct for the known radium/uranium disequilibrium of the NBL standards (George and others, 1983). It was assumed that the KUT concentrations were to be assigned to the models as if the ores used in the construction of the models were in secular equilibrium throughout their respective decay chains.

A linear regression was performed to relate the corrected count rates to the corrected laboratory assay concentrations. In the regression, both count rates and assay values were adjusted to form a set of collinear points. The adjusted assay concentrations derived from this regression are the newly assigned concentrations for the spectral gamma-ray borehole calibration models.

1.4 COMPARISON WITH NaI DATA

Because of the widespread use of sodium iodide (NaI) detectors in industry logging applications, a series of measurements was obtained using the filtered 1.5-inch-by-2.0-inch NaI detector from the Calibration Facilities Monitoring System (CFMS) (George and others, 1983). These measurements were then used to calibrate the detector at each of the various field sites. Results of these calibrations were used to verify the self-consistency of the concentration assignments and to check the adequacy of the assignments for use in calibrating NaI detectors.

2.0 LABORATORY ASSAY DATA

2.1 SAMPLE ACQUISITION AND PREPARATION

At the time of each model's construction, samples were taken from the concrete pour and were prepared for analysis by the Bendix Geochemistry Laboratory. This preparation involved curing the samples, crushing them, driving off the free moisture, and sealing them in cans to enable radon equilibrium to occur. Between 10 and 24 samples from each model were included in this study.

2.2 DATA COLLECTION

The current set of assays was run between 14 March and 22 August 1983. Each sample was assayed for its concentrations of potassium, uranium, and thorium (see Appendix A, Laboratory Assay Data). The assays were performed on a lithium-drifted germanium [Ge(Li)] detector. In most cases, the concentration of potassium was based on the 1461-keV (K-40) peak, the concentration of

uranium on the 1765-keV (Bi-214) peak, and the concentration of thorium on the 2615-keV (Tl-208) peak. In certain cases, a secondary peak was used to determine the concentrations (Dechant, in preparation).

The Ge(Li) detector was calibrated using the NBL 100A Series standards. This calibration represents the link by which the newly assigned concentrations can be traced to the national standards.

2.3 DATA REDUCTION

As mentioned above, a correction to the assayed uranium concentration was made. This correction was necessary because the reported concentration was determined from the radium-daughter peak at 1765 keV and the NBL standards are not in radium/uranium equilibrium. The ratio of radium to uranium for the NBL standards was reported to be 3.44×10^{-7} gram Ra-226 per gram U (Trahey and others, 1982). The ratio assumed for the central zones of the models was 3.376×10^{-7} gram Ra-226 per gram U, which is the value at equilibrium (George and others, 1983).

Data from the laboratory assays are summarized in Table 2-1. The concentrations of potassium, uranium, and thorium for each model are the average values reported for the samples taken from that model. The uncertainty associated with each value is the maximum obtained by combining the effects of two potential factors. First, an uncertainty was determined from the variance of the reported assay values about their average. Second, an uncertainty was calculated from the reported uncertainties in the laboratory assay value. The first method tends to produce rather inaccurate estimates of the uncertainty for sets of data with fewer than 30 samples. Since we have only between 10 and 24 samples from each model, it follows that we do not expect the uncertainty calculated by this method to be a good estimate. The uncertainties reported by the Geochemistry Laboratory provided a reliable lower boundary which prevented us from underestimating the uncertainty in the assay values. However, use of the latter method alone produces low values in those models having a relatively large degree of inhomogeneity in their enriched zones.

One further note: The Geochemistry Laboratory did not report values for several of the samples, but instead reported them as being below a detection limit. This usually occurred when the sample had a near-background concentration of one radioelement and a relatively high concentration of another radioelement having a higher energy photopeak, which raised the Compton-scattered background flux levels and made it difficult to report an accurate value for the lower energy photopeak. If we assume that the detection limit reported by the laboratory is in fact correct, then all we know about the value is that it lies somewhere between zero and the detection limit. If we then assume a uniform distribution of these possible values, the average value must be equal to one-half the detection limit, and its uncertainty is 68 percent of the average. These values were used where necessary to determine the average values and uncertainties cited in Table 2-1.

Table 2-1. Laboratory Assay Data

Model	Number of Samples	K (%)*	eU (ppm)*	eTh (ppm)*
K	10	6.64 ± 0.18	3.03 ± 0.46	1.35 ± 0.90
U	10	1.16 ± 0.12	495.00 ± 15.00	3.00 ± 1.90
T	10	1.36 ± 0.18	25.80 ± 2.70	497.00 ± 21.00
KW	24	4.47 ± 0.22	360.00 ± 12.00	240.40 ± 7.80
BK	15	6.48 ± 0.17	2.99 ± 0.10	0.89 ± 0.59
BU	15	1.27 ± 0.13	590.00 ± 47.00	4.40 ± 2.10
BT	15	1.20 ± 0.16	28.00 ± 3.60	536.00 ± 16.00
BM	15	5.15 ± 0.14	395.00 ± 23.00	368.70 ± 9.10
CBK	10	6.07 ± 0.26	3.60 ± 0.54	1.40 ± 0.93
CBU	10	1.38 ± 0.15	529.00 ± 16.00	4.50 ± 1.20
CBT	10	1.34 ± 0.08	33.30 ± 1.90	643.00 ± 11.00
CBM	10	4.94 ± 0.25	388.00 ± 19.00	449.00 ± 14.00
TBK	10	6.50 ± 0.18	3.56 ± 0.50	0.92 ± 0.62
TBU	10	1.21 ± 0.11	517.00 ± 28.00	2.50 ± 2.00
TBT	10	1.09 ± 0.11	32.60 ± 2.80	612.70 ± 8.30
TBM	10	5.13 ± 0.18	388.00 ± 27.00	458.90 ± 7.80
GBK	10	6.07 ± 0.13	2.77 ± 0.92	1.10 ± 0.64
GBU	10	1.38 ± 0.11	558.00 ± 33.00	5.30 ± 1.90
GBT	10	1.14 ± 0.12	31.80 ± 1.70	623.00 ± 12.00
GBM	10	4.74 ± 0.20	391.00 ± 16.00	436.00 ± 11.00
MBK	15	6.65 ± 0.21	3.23 ± 0.40	1.13 ± 0.76
MBU	15	1.04 ± 0.14	581.00 ± 46.00	2.00 ± 1.50
MBT	15	1.21 ± 0.11	30.30 ± 3.20	503.00 ± 15.00
MBM	15	5.04 ± 0.22	394.00 ± 19.00	354.60 ± 8.40
RBK	15	6.63 ± 0.16	3.48 ± 0.69	1.23 ± 0.82
RBU	15	1.23 ± 0.13	584.00 ± 32.00	4.70 ± 2.10
RBT	15	1.18 ± 0.22	31.00 ± 12.00	497.00 ± 15.00
RBM	15	5.28 ± 0.22	383.00 ± 20.00	379.00 ± 15.00
SBK	12	6.05 ± 0.17	3.52 ± 0.30	1.33 ± 0.89
SBU	15	1.31 ± 0.18	593.00 ± 50.00	4.20 ± 2.30
SBT	15	1.32 ± 0.15	32.20 ± 4.20	539.00 ± 21.00
SBM	15	4.87 ± 0.24	386.00 ± 14.00	350.00 ± 11.00

*Uncertainties cited are 1 standard deviation (68 percent confidence interval).

3.0 MOISTURE MEASUREMENTS

The moisture in the models was measured using an epithermal neutron-neutron probe (George and others, 1983) from the Calibration Facilities Monitoring System. A profile of each model was made in a stop-and-go fashion, counting for approximately 15 seconds every 0.1 foot through the model. The average count rate in each enriched zone was determined by inspecting the plot of the profile (see Appendix B, Neutron Profiles).

3.1 NEUTRON PROBE CALIBRATION

The neutron probe was calibrated in the M-barrels, a set of moisture models located at the Grand Junction site (Duray, 1977). The relationship between the moisture in the model and the neutron probe count rate is represented by the equation

$$\rho_w = 0.5208 - (3.156\text{x}10^{-4})N + (5.53\text{x}10^{-8})N^2$$

where ρ_w is the partial density of water in the concrete in the models (in g/cc) and N is the epithermal neutron count rate measured by the probe (in cps).

A problem arose with respect to calibration in the M-barrels when an unexpected and unexplained change in the count rate measured in the M2 barrel occurred during the period 16 June to 10 September 1981 (George and others, 1983). Since this change in the M2 barrel was detected, the M-barrels have not been used for calibration purposes. Instead, the earlier calibration factors have been used because the neutron probe had been the most stable and unchanging of our probes, and no change was noted for the M1 and M3 barrels.

However, in August 1983, prior to acquisition of data at the Reno, Spokane, and Casper sites, it was noticed that the probe was emitting excessive background noise. The probe was repaired, but a subsequent change in the stability count rate was observed. This change in the count rate was corrected using the equation

$$N_c = (1.031)N$$

where N_c is the corrected epithermal neutron count rate. The factor (1.031) used to multiply the observed epithermal neutron count rate was determined as the ratio of the epithermal neutron stability measurements taken before and after the change occurred (see Section 7.0). As a measure of the adequacy of this correction, the moisture measured in the K model before repairs were made in the probe was 0.2113 g/cc while the moisture measured after the repairs was 0.2092 g/cc, a difference of only 1 percent; at the same time, the observed count rate changed from 1013 cps to 991 cps, a difference of 2.2 percent. Thus, the correction maintains the uncertainty in the moisture value to well within the 8 percent uncertainty that has been assumed for all the moisture values (see Section 4.1.2).

3.2 MOISTURE DATA REDUCTION

Table 3-1 presents the corrected epithermal neutron count rates as measured in the models with the neutron probe. No data from the Morgantown site were collected with the neutron probe during this study because of difficulties encountered with the multichannel analyzer (MCA) in the Calibration Facilities Monitoring System. The data for the Morgantown models cited in Table 3-1 were collected during a previous site visit in 1982 (George and others, 1983).

Table 3-1. Moisture Calculations

Model	Corrected Epithermal Neutron Count Rate (cps)	Partial Density H_2O (g/cc)	Dry Bulk Density (g/cc)	Dry Base Moisture (wt-fraction)
K	960	0.2688	1.86	0.1445
U	935	0.2741	1.89	0.1450
T	930	0.2751	1.88	0.1463
KW	983	0.2640	1.86	0.1419
BK	1052	0.2500	1.81	0.1381
BU	1090	0.2425	1.91	0.1270
BT	1085	0.2435	1.91	0.1275
BM	1045	0.2514	1.88	0.1337
CBK	1026*	0.2552	1.81	0.1410
CBU	1108*	0.2390	1.91	0.1251
CBT	1113*	0.2380	1.91	0.1246
CBM	1040*	0.2524	1.88	0.1342
TBK	985	0.2636	1.81	0.1456
TBU	1065	0.2474	1.87	0.1323
TBT	1087	0.2431	1.94	0.1253
TBM	1018	0.2568	1.85	0.1388
GBK	990	0.2626	1.81	0.1451
GBU	1082	0.2441	1.88	0.1298
GBT	1060	0.2484	1.93	0.1287
GBM	1015	0.2574	1.87	0.1377
MBK	1052	0.2500	1.86	0.1344
MBU	1105	0.2396	1.89	0.1268
MBT	1107	0.2392	1.92	0.1246
MBM	1045	0.2514	1.87	0.1344
RBK	1028*	0.2548	1.84	0.1385
RBU	1100*	0.2406	1.88	0.1280
RBT	1093*	0.2419	1.90	0.1273
RBM	1040*	0.2524	1.87	0.1350
SBK	1070*	0.2464	1.82	0.1354
SBU	1103*	0.2400	1.90	0.1263
SBT	1140*	0.2329	1.92	0.1213
SBM	1045*	0.2514	1.87	0.1344

*Measurement taken after probe repairs; correction factor (cf. Section 3.1) applied.

Also listed in Table 3-1 are the dry bulk density for each model and the dry base moisture fraction of the model. Dry bulk density was determined by the Geochemistry Laboratory, except in the case of models MBU, MBT, MBM, RBM, SBT, SBK, and SBM for which density data from the laboratory were unavailable. For these models, the average of the density values from all other models of the particular model type was used, i.e., for model MBU the average dry bulk density of all BU-type models was used. The dry base moisture fraction is defined as the ratio of the partial density of water to the dry bulk density.

4.0 HIGH-PURITY GERMANIUM DETECTOR DATA

A high-purity germanium (HPGe) detector was used to acquire data from the enriched zones in the calibration models (Murri and others, 1983). A spectrum was collected at a stationary position at the center of each enriched zone. Count rates in three photopeaks of interest were determined: 1461 keV (potassium), 1765 keV (uranium), and 2615 keV (thorium). The net areas under the peaks divided by the live time of the acquisition are the observed KUT count rates for the model.

Acquisition of a single, fixed-position spectrum rather than a profile measurement of the entire model is standard procedure in KUT calibration work. In this study, the spectrum in each enriched zone was acquired for 5000 seconds of MCA live time. In order to determine dead time, the signal from a random pulser was mixed with the gamma-ray signals and was adjusted to produce a peak count rate equal to 1.5 percent of the total count rate from the spectrum being measured. The spectral data were stored on magnetic tape and later analyzed on a local computer system. The raw data were smoothed using a five-point smoothing algorithm, and the peak centroids were determined using the central-difference method. The total count rate in the peak, the net count rate in the peak (Compton background subtracted), and the uncertainty in the net count rate (Murri and others, 1983) were then calculated. The uncertainty was calculated by assuming Poisson statistics for the count-rate data. This analysis was performed on several peaks in addition to the pulser peak and the three gamma-ray spectral peaks described above. Results for the three gamma-ray peaks of interest are summarized in Table 4-1; additional HPGe data are contained in Appendix C.

4.1 CORRECTIONS TO THE HPGe MEASUREMENTS

Theory predicts that the number of gamma rays emitted per second by a radioactive element is directly proportional to the concentration of the element in the host matrix. However, several factors combine to make the relationship between the observed gamma-ray count rate in a borehole environment and the concentration of the associated radioelement nonlinear, among them detector dead time, presence of moisture, poor detector resolution, and the effects of borehole size, fluid, and casing (Wilson, 1981).

4.1.1 System Dead Time

The count rate measured in a peak must be adjusted to reflect the amount of time the system had been unable to process input signals during the period of acquisition. The dead-time correction for the HPGe crystal detector is measured by comparing the area of the spectral peak produced by the signal from the random pulser with the number of counts actually output by the pulser, as counted on a scaler. Since the pulser rate is adjusted to match an 'average' gamma-ray peak in the spectrum, the fractional losses from the pulser peak are assumed to be the same as those from the natural gamma-ray peaks (Murri and others, 1983).

Table 4-1. Raw HPGe Count-Rate Data

Model	1461-keV Potassium Peak Count Rate (cps)*	1765-keV 'Uranium' Peak Count Rate (cps)*	2615-keV 'Thorium' Peak Count Rate (cps)*
K	4.921 ± 0.032	0.117 ± 0.005	0.066 ± 0.004
U	0.938 ± 0.034	19.549 ± 0.067	0.167 ± 0.006
T	1.346 ± 0.027	1.054 ± 0.023	12.347 ± 0.051
KW	3.710 ± 0.045	14.670 ± 0.060	6.102 ± 0.036
BK	5.170 ± 0.033	0.148 ± 0.006	0.023 ± 0.002
BU	0.972 ± 0.037	23.696 ± 0.075	0.148 ± 0.006
BT	1.399 ± 0.027	1.328 ± 0.025	13.935 ± 0.054
BM	4.211 ± 0.048	16.027 ± 0.064	9.178 ± 0.044
CBK	4.992 ± 0.032	0.148 ± 0.006	0.026 ± 0.002
CBU	1.061 ± 0.036	21.381 ± 0.071	0.159 ± 0.006
CBT	1.432 ± 0.030	1.448 ± 0.027	16.032 ± 0.058
CBM	4.095 ± 0.048	15.524 ± 0.062	10.803 ± 0.047
TBK	5.097 ± 0.032	0.143 ± 0.006	0.021 ± 0.002
TBU	1.063 ± 0.036	21.582 ± 0.071	0.159 ± 0.006
TBT	1.457 ± 0.030	1.430 ± 0.027	16.103 ± 0.058
TBM	4.125 ± 0.048	15.522 ± 0.062	10.855 ± 0.048
GBK	5.010 ± 0.032	0.138 ± 0.005	0.024 ± 0.002
GBU	1.099 ± 0.036	21.821 ± 0.071	0.163 ± 0.006
GBT	1.435 ± 0.029	1.449 ± 0.027	16.106 ± 0.058
GBM	4.210 ± 0.048	15.666 ± 0.063	11.001 ± 0.048
MBK	5.194 ± 0.033	0.121 ± 0.005	0.026 ± 0.002
MBU	1.016 ± 0.037	23.725 ± 0.074	0.152 ± 0.006
MBT	1.434 ± 0.029	1.254 ± 0.025	13.443 ± 0.053
MBM	4.211 ± 0.048	15.695 ± 0.062	8.958 ± 0.043
RBK	5.064 ± 0.032	0.129 ± 0.005	0.026 ± 0.002
RBU	0.958 ± 0.039	23.340 ± 0.074	0.153 ± 0.006
RBT	1.414 ± 0.028	1.281 ± 0.026	13.309 ± 0.053
RBM	4.168 ± 0.049	15.534 ± 0.063	9.024 ± 0.044
SBK	5.205 ± 0.033	0.149 ± 0.006	0.026 ± 0.002
SBU	0.977 ± 0.037	23.166 ± 0.075	0.152 ± 0.006
SBT	1.439 ± 0.029	1.273 ± 0.024	13.839 ± 0.054
SBM	4.104 ± 0.047	15.276 ± 0.061	8.945 ± 0.043

*Uncertainties cited are 1 standard deviation (68 percent confidence interval).

Table 4-2 lists the dead-time correction factors used in this study. These factors were determined using the equation

$$F_d = P_i/P_o$$

where F_d is the dead-time correction factor, P_i is the number of pulses output from the random pulser, and P_o is the number of counts recorded in the pulser peak in the MCA spectrum.

Table 4-2. Dead-Time Correction Factors

Model	Count Rate in Pulser Peak (cps)*	Count Rate Output from Pulser (cps)*	Dead-Time Correction Factor*
K	4.509 ± 0.030	4.518 ± 0.030	1.0020 ± 0.0005
U	61.028 ± 0.110	64.219 ± 0.113	1.0523 ± 0.0004
T	24.754 ± 0.073	25.300 ± 0.071	1.0221 ± 0.0009
KW	64.158 ± 0.116	67.412 ± 0.116	1.0507 ± 0.0005
BK	4.153 ± 0.029	4.165 ± 0.029	1.0029 ± 0.0006
BU	59.920 ± 0.112	63.791 ± 0.113	1.0646 ± 0.0006
BT	24.667 ± 0.073	25.281 ± 0.071	1.0249 ± 0.0009
BM	66.895 ± 0.118	70.786 ± 0.119	1.0582 ± 0.0005
CBK	2.335 ± 0.022	2.342 ± 0.022	1.0029 ± 0.0010
CBU	101.609 ± 0.144	107.671 ± 0.147	1.0597 ± 0.0004
CBT	46.973 ± 0.099	48.372 ± 0.098	1.0298 ± 0.0005
CBM	103.195 ± 0.147	109.588 ± 0.148	1.0620 ± 0.0004
TBK	5.447 ± 0.033	5.453 ± 0.033	1.0010 ± 0.0001
TBU	114.763 ± 0.153	121.545 ± 0.156	1.0591 ± 0.0004
TBT	58.517 ± 0.111	60.197 ± 0.110	1.0287 ± 0.0005
TBM	114.151 ± 0.153	121.231 ± 0.156	1.0620 ± 0.0004
GBK	2.347 ± 0.022	2.355 ± 0.022	1.0033 ± 0.0012
GBU	69.088 ± 0.121	72.849 ± 0.121	1.0544 ± 0.0006
GBT	27.104 ± 0.075	27.778 ± 0.075	1.0249 ± 0.0007
GBM	71.544 ± 0.125	75.590 ± 0.123	1.0565 ± 0.0006
MBK	6.326 ± 0.036	6.333 ± 0.036	1.0010 ± 0.0003
MBU	109.160 ± 0.150	116.396 ± 0.153	1.0663 ± 0.0004
MBT	28.927 ± 0.079	29.682 ± 0.077	1.0261 ± 0.0008
MBM	94.249 ± 0.140	99.865 ± 0.141	1.0596 ± 0.0004
RBK	7.841 ± 0.040	7.856 ± 0.040	1.0019 ± 0.0002
RBU	39.051 ± 0.091	41.533 ± 0.091	1.0636 ± 0.0008
RBT	34.308 ± 0.085	35.177 ± 0.084	1.0253 ± 0.0007
RBM	39.298 ± 0.093	41.399 ± 0.091	1.0534 ± 0.0008
SBK	12.022 ± 0.049	12.046 ± 0.049	1.0020 ± 0.0003
SBU	114.137 ± 0.156	121.728 ± 0.156	1.0665 ± 0.0004
SBT	52.429 ± 0.104	53.711 ± 0.104	1.0245 ± 0.0005
SBM	114.986 ± 0.154	121.643 ± 0.156	1.0579 ± 0.0004

*Uncertainties cited are 1 standard deviation (68 percent confidence interval).

The uncertainties associated with the dead-time correction factors were calculated using the uncertainty in P_o as reported by the reduction program and assuming Poisson statistics for P_i. The covariance between the pulses output from the pulser and the pulses registered in the spectral peak was also taken into account. This gives a final equation for the uncertainty in the dead-time correction factor of

$$\sigma F_d = F_d \sqrt{(\sigma P_o / P_o)^2 - 1/P_i}$$

This equation is an approximation, assuming that the covariance is equal to the fraction of counts not lost to dead time, i.e.,

$$\sigma(P_o,P_i) = (P_o/P_i)[\sigma(P_o)\sigma(P_i)] \approx (P_o/P_i)\sigma^2(P_i)$$

where $\sigma(P_o,P_i)$ is the covariance of P_o and P_i. Even though the final equation used is only an approximation, the uncertainty introduced by this term into the final value is very small; hence, the uncertainty due to the approximation is insignificant.

4.1.2 Moisture

Another correction which must be made before the spectral peak count rate is proportional to the radioelement concentration is due to the water in the pore spaces of the concrete. The concentrations assigned on the basis of the assays were determined from dry samples; however, moisture exists in the models and the presence of moisture attenuates the gamma-ray flux through the concrete. To relate the 'wet' gamma-ray peak count rate to the 'dry' concentrations requires a correction factor based on the amount of moisture in the pore spaces of the concrete.

The effect of moisture on gamma-ray flux varies depending on the energy of the gamma rays. The correction is represented by the ratio of the wet-linear-attenuation coefficient to the dry-linear-attenuation coefficient, where 'wet' implies the actual concrete and 'dry' implies the same concrete with zero free moisture content (Wilson and Stromswold, 1981). Linear attenuation coefficients are calculated as the product of the density of the concrete in the models and the mass attenuation coefficient for the material in question.

Therefore,

$$L_d = \rho_d\mu_d$$

$$L_w = \rho_d\mu_d + \rho_w\mu_w$$

where L_d is the dry linear attenuation coefficient, ρ_d is the dry bulk density of the concrete in the models, μ_d is the mass attenuation coefficient for dry concrete, L_w is the wet linear attenuation coefficient, ρ_w is the partial density of water, and μ_w is the mass attenuation coefficient for water.

The mass attenuation coefficients for water and concrete were determined from a regression of the values cited in the Radiological Health Handbook (Department of Health, Education, and Welfare, 1970). The coefficient for a given material was calculated as a function of gamma-ray energy through a regression analysis. Table 4-3 lists the mass attenuation coefficients determined for water and for concrete; Table 4-4 lists the mass attenuation values calculated for the coefficients for these two materials at energies of 1461 keV, 1765 keV, 2204 keV, and 2615 keV. The value for the mass attenuation of the 2204-keV peak was included for use with the NaI detector system (see Section 6.0).

The correction factor for moisture in the model can be expressed as

$$F_m = 1 + (\mu_w/\mu_d)M$$

where F_m is the moisture correction factor and M is the dry base moisture in the model. Table 4-5 lists the moisture correction factors for the peak count rates from the HPGe detector.

It was assumed that the uncertainty in the dry base moisture value, M, was less than 8 percent, based roughly on the repeatability of the neutron profile measurements and on the accuracy of the dry bulk density values determined by the Geochemistry Laboratory. It was also assumed that the uncertainty in the determination of the mass attenuation coefficients as a function of gamma-ray energy (~2 percent) was minimal in comparison and could be ignored. Thus, the uncertainty in the moisture correction factor was based on the two former factors and was calculated from the equation

$$\sigma F_m = M(\mu_w/\mu_d)0.08$$

It should be noted that an assumed uncertainty of 8 percent in the value of M gives a calculated uncertainty of only about 1 percent in the value of F_m; therefore, the assumed value of 8 percent is not critical.

Table 4-3. Mass Attenuation Regression Coefficients*

Coefficient	Concrete	Water
b_0	0.105916	0.117202
b_1	-0.0558144	-0.0612800
b_2	0.0156889	0.0170097
b_3	-0.00159106	-0.00172322

*$\mu = b_0 + b_1E + b_2E^2 + b_3E^3$, where μ is the mass attenuation coefficient (in cm^2/g) and E is the gamma-ray energy (in MeV).

Table 4-4. Mass Attenuation Values

Energy (MeV)	Concrete (cm^2/g)	Water (cm^2/g)
2.615	0.03879	0.04246
2.204	0.04208	0.04632
1.765	0.04753	0.05256
1.461	0.05290	0.05861

Table 4-5. Moisture Correction Factors

Model	Potassium Peak*	'Uranium' Peak*	'Thorium' Peak*
K	1.160 ± 0.013	1.160 ± 0.013	1.158 ± 0.013
U	1.161 ± 0.013	1.160 ± 0.013	1.159 ± 0.013
T	1.162 ± 0.013	1.162 ± 0.013	1.160 ± 0.013
KW	1.157 ± 0.013	1.157 ± 0.013	1.155 ± 0.012
BK	1.153 ± 0.012	1.153 ± 0.012	1.151 ± 0.012
BU	1.141 ± 0.011	1.140 ± 0.011	1.138 ± 0.011
BT	1.141 ± 0.011	1.141 ± 0.011	1.140 ± 0.011
BM	1.148 ± 0.011	1.148 ± 0.011	1.146 ± 0.011
CBK	1.156 ± 0.012	1.156 ± 0.012	1.154 ± 0.012
CBU	1.139 ± 0.012	1.138 ± 0.012	1.137 ± 0.012
CBT	1.138 ± 0.011	1.138 ± 0.011	1.136 ± 0.011
CBM	1.149 ± 0.012	1.148 ± 0.012	1.147 ± 0.012
TBK	1.161 ± 0.013	1.161 ± 0.013	1.159 ± 0.013
TBU	1.147 ± 0.012	1.146 ± 0.012	1.144 ± 0.012
TBT	1.139 ± 0.011	1.139 ± 0.011	1.137 ± 0.011
TBM	1.154 ± 0.012	1.154 ± 0.012	1.152 ± 0.012
GBK	1.161 ± 0.013	1.160 ± 0.013	1.158 ± 0.013
GBU	1.144 ± 0.011	1.144 ± 0.011	1.142 ± 0.011
GBT	1.143 ± 0.011	1.142 ± 0.011	1.141 ± 0.011
GBM	1.153 ± 0.012	1.152 ± 0.012	1.150 ± 0.012
MBK	1.149 ± 0.012	1.149 ± 0.012	1.147 ± 0.012
MBU	1.140 ± 0.011	1.140 ± 0.011	1.138 ± 0.011
MBT	1.138 ± 0.011	1.138 ± 0.011	1.136 ± 0.011
MBM	1.149 ± 0.012	1.149 ± 0.012	1.147 ± 0.012
RBK	1.153 ± 0.012	1.153 ± 0.012	1.152 ± 0.012
RBU	1.142 ± 0.011	1.141 ± 0.011	1.140 ± 0.011
RBT	1.141 ± 0.011	1.140 ± 0.011	1.139 ± 0.011
RBM	1.150 ± 0.012	1.149 ± 0.012	1.147 ± 0.012
SBK	1.150 ± 0.012	1.150 ± 0.012	1.148 ± 0.012
SBU	1.140 ± 0.011	1.140 ± 0.011	1.138 ± 0.011
SBT	1.134 ± 0.011	1.134 ± 0.011	1.133 ± 0.011
SBM	1.149 ± 0.012	1.149 ± 0.012	1.147 ± 0.012

*Uncertainties cited are 1 standard deviation (68 percent confidence interval).

4.1.3 Detector Resolution

An additional correction to the potassium count rate for contributions from an actinium-228 (a thorium daughter) gamma ray was also required because the HPGe detector does not have the resolution necessary to distinguish between actinium-228 at 1459 keV and potassium-40 at 1461 keV. The correction is made assuming that the actinium-228 and bismuth-212 in the thorium decay chain are in equilibrium, and that the areas of the two peaks are proportional to each other. The correction has the form

$$K_t = K_a - T_a(I1459/I2615)(DE1459/DE2615)(L2615/L1459)(1/BR)$$
$$= K_a - T_a 0.0317$$

where K_t is the thorium-corrected potassium peak count rate, K_a is the moisture-corrected potassium peak count rate, T_a is the moisture-corrected thorium peak count rate, I1459 is the absolute intensity of the 1459-keV gamma ray (gammas per decay of Ac-228), I2615 is the absolute intensity of the 2615-keV gamma ray, DE is the detector efficiency (determined at the two energies of interest), L is the wet linear attenuation coefficient for the concrete of the model, and BR is the alpha-decay branching ratio for bismuth-212 (equal to 0.36) since all of the thorium decays do not eventually produce a thallium atom (as is virtually the case for actinium). The resultant uncertainty in determining this factor (0.0317) is roughly 10 percent (George and others, in preparation).

4.2 CORRECTED HPGe COUNT RATES

The observed peak count rates, obtained with the HPGe detector, were corrected using the factors described in Section 4.1; these corrected data are listed in Table 4-6. The uncertainties were calculated using the uncertainties derived from each correction factor and the uncertainties in the observed count rates.

Table 4-6. Corrected HPGe Count-Rate Data

Model	1461-keV Potassium Peak Count Rate (cps)*	1765-keV 'Uranium' Peak Count Rate (cps)*	2615-keV 'Thorium' Peak Count Rate (cps)*
K	5.713 ± 0.073	0.135 ± 0.006	0.077 ± 0.004
U	1.138 ± 0.043	23.859 ± 0.276	0.203 ± 0.008
T	1.134 ± 0.064	1.251 ± 0.031	14.635 ± 0.173
KW	4.275 ± 0.078	17.825 ± 0.207	7.404 ± 0.091
BK	5.974 ± 0.074	0.171 ± 0.007	0.027 ± 0.003
BU	1.174 ± 0.047	28.754 ± 0.297	0.179 ± 0.008
BT	1.119 ± 0.067	1.552 ± 0.033	16.259 ± 0.171
BM	4.742 ± 0.087	19.379 ± 0.209	11.083 ± 0.122
CBK	5.774 ± 0.072	0.171 ± 0.007	0.030 ± 0.003
CBU	1.284 ± 0.046	25.992 ± 0.281	0.193 ± 0.008
CBT	1.084 ± 0.076	1.696 ± 0.035	18.761 ± 0.193
CBM	4.576 ± 0.091	18.925 ± 0.210	13.153 ± 0.146
TBK	5.922 ± 0.076	0.167 ± 0.007	0.025 ± 0.002
TBU	1.284 ± 0.045	26.189 ± 0.280	0.193 ± 0.008
TBT	1.109 ± 0.077	1.674 ± 0.035	18.828 ± 0.193
TBM	4.631 ± 0.092	19.006 ± 0.216	13.273 ± 0.151
GBK	5.831 ± 0.075	0.161 ± 0.007	0.028 ± 0.003
GBU	1.318 ± 0.045	26.299 ± 0.277	0.196 ± 0.008
GBT	1.083 ± 0.076	1.696 ± 0.036	18.823 ± 0.198
GBM	4.700 ± 0.093	19.063 ± 0.215	13.369 ± 0.152
MBK	5.970 ± 0.072	0.139 ± 0.006	0.030 ± 0.003
MBU	1.229 ± 0.047	28.830 ± 0.297	0.184 ± 0.008
MBT	1.178 ± 0.067	1.463 ± 0.032	15.667 ± 0.162
MBM	4.779 ± 0.088	19.093 ± 0.211	10.884 ± 0.123
RBK	5.848 ± 0.073	0.149 ± 0.007	0.030 ± 0.003
RBU	1.157 ± 0.049	28.322 ± 0.295	0.185 ± 0.008
RBT	1.161 ± 0.066	1.498 ± 0.033	15.540 ± 0.164
RBM	4.699 ± 0.088	18.798 ± 0.210	10.905 ± 0.124
SBK	5.994 ± 0.073	0.171 ± 0.007	0.030 ± 0.003
SBU	1.181 ± 0.047	28.144 ± 0.290	0.184 ± 0.008
SBT	1.162 ± 0.067	1.478 ± 0.031	16.052 ± 0.162
SBM	4.642 ± 0.086	18.553 ± 0.206	10.850 ± 0.123

*Uncertainties cited are 1 standard deviation (68 percent confidence interval).

5.0 CONCENTRATION ASSIGNMENTS

5.1 REGRESSION PROCEDURE

The newly assigned concentrations for the borehole calibration models (Table 5-1) were determined by a regression of the corrected peak count rates versus the average assay concentrations. A method of weighting, based on the uncertainties in the corrected count rates and in the laboratory assay data, was used in this regression, and is detailed in the paragraphs that follow.

Table 5-1. Final Assigned Concentrations

Model	Potassium (%)*	Uranium (ppm)*	Thorium (ppm)*
K	6.24 ± 0.10	2.76 ± 0.13	2.53 ± 0.14
U	1.22 ± 0.05	488.20 ± 8.00	6.65 ± 0.27
T	1.24 ± 0.07	25.39 ± 0.70	485.60 ± 6.80
KW	4.59 ± 0.10	361.30 ± 6.00	244.60 ± 3.60
BK	6.45 ± 0.10	3.10 ± 2.50	0.89 ± 0.10
BU	1.27 ± 0.06	583.20 ± 8.90	5.91 ± 0.27
BT	1.21 ± 0.08	31.36 ± 0.76	538.30 ± 7.00
BM	5.12 ± 0.12	393.10 ± 6.10	367.40 ± 5.00
CBK	6.21 ± 0.10	3.48 ± 0.15	1.00 ± 0.10
CBU	1.38 ± 0.05	527.30 ± 8.40	6.30 ± 0.28
CBT	1.26 ± 0.12	34.26 ± 0.84	626.90 ± 8.30
CBM	4.93 ± 0.11	384.00 ± 6.10	437.10 ± 5.90
TBK	6.40 ± 0.11	3.40 ± 0.15	0.83 ± 0.07
TBU	1.36 ± 0.06	530.50 ± 8.30	6.33 ± 0.27
TBT	1.16 ± 0.10	33.87 ± 0.82	619.60 ± 8,60
TBM	5.02 ± 0.12	385.50 ± 6.20	445.20 ± 6.40
GBK	6.23 ± 0.11	3.25 ± 0.15	0.93 ± 0.10
GBU	1.41 ± 0.05	534.00 ± 8.20	6.47 ± 0.27
GBT	1.16 ± 0.09	33.99 ± 0.87	623.40 ± 8.40
GBM	5.00 ± 0.12	386.89 ± 6.20	441.60 ± 6.20
MBK	6.46 ± 0.10	2.85 ± 0.13	1.00 ± 0.10
MBU	1.29 ± 0.06	584.60 ± 8.90	5.97 ± 0.27
MBT	1.25 ± 0.08	29.69 ± 0.74	517.10 ± 6.60
MBM	5.13 ± 0.11	387.50 ± 6.10	359.40 ± 5.10
RBK	6.37 ± 0.10	3.04 ± 0.15	1.00 ± 0.10
RBU	1.24 ± 0.06	574.70 ± 8.80	6.11 ± 0.27
RBT	1.24 ± 0.08	30.38 ± 0.75	512.70 ± 6.70
RBM	5.10 ± 0.11	381.30 ± 6.10	362.40 ± 4.90
SBK	6.39 ± 0.10	3.48 ± 0.16	1.00 ± 0.10
SBU	1.28 ± 0.05	571.00 ± 8.70	6.07 ± 0.27
SBT	1.27 ± 0.08	30.02 ± 0.72	532.10 ± 6.60
SBM	4.99 ± 0.11	377.00 ± 6.00	358.20 ± 4.90

*Uncertainties cited are 1 standard deviation (68 percent confidence interval).

The count-rate data, after all corrections had been applied, were fitted to the laboratory assay data through a regression procedure. It was decided to use a regression that weighted the results based upon the calculated uncertainties in both data sets (York, 1966). This regression minimized the sum

$$S = \sum_i [w(X_i)(x_i - X_i)^2] + \sum_i [w(Y_i)(y_i - Y_i)^2]$$

where X_i is the corrected peak count rate, Y_i is the laboratory assay concentration, $w(X_i)$ is a weighting factor for the count-rate data (equal to the reciprocal of its uncertainty squared), $w(Y_i)$ is a similar weighting factor for the assay concentration data, and x_i and y_i are the adjusted values which

are chosen such that

$$y_i = kx_i$$

where k is the calibration coefficient (k-factor) of the instrument. If it is assumed, as theory predicts, that the radioelement concentration in the model is directly proportional to the corrected count rate, then the values of x_i and y_i give us the best estimate of the 'true' count rates and concentrations. To minimize the sum, S, subject to the constraint that the adjusted concentrations are proportional to the adjusted count rates, the adjusted value of x_i must be calculated from the equation

$$x_i = X_i - \{kw(Y_i)(kX_i - Y_i)/[k^2 w(Y_i) + w(X_i)]\}$$

The uncertainty in each x_i is then calculated using the uncertainty in the original X_i as well as the uncertainty in the adjustment. The uncertainty in the adjusted concentrations is based upon the uncertainty in the adjusted count rate and the uncertainty in the calibration coefficient, k.

Figures 5-1, 5-2, and 5-3 show the regression lines calculated for the potassium, uranium, and thorium data, respectively, based on the data used for this study and the uncertainties in the data.

5.2 DISCUSSION OF RESULTS

A comparison of the results of this work with those of a previous investigation based on total-count measurements (George and others, 1983) shows that these new uranium assignments for the U models are consistently higher by 2 to 6 percent. This discrepancy cannot be explained solely on the basis of statistical uncertainties in either the laboratory assay values or the in-situ count-rate data. Although the present study used slightly different laboratory assay values than did the previous work (the same physical samples, but measured on two separate occasions by the Geochemistry Laboratory), the assay values repeated within the statistical uncertainties determined for them. Hence, the two sets of assays can be considered statistically equivalent (Table 5-2).

Table 5-2. Comparison of Laboratory Assay Concentrations

	Laboratory Assay Uranium Concentration (ppm)*	
Model	Total-Count Study**	Present Study
U	499 ± 9	495 ± 15
BU	575 ± 43	590 ± 47
CBU	513 ± 11	529 ± 16
TBU	518 ± 31	517 ± 28
GBU	533 ± 30	558 ± 33
MBU	583 ± 52	581 ± 46
RBU	577 ± 40	584 ± 32
SBU	586 ± 46	593 ± 50

*Uncertainties cited are one standard deviation (68 percent confidence interval).

**George and others, 1983.

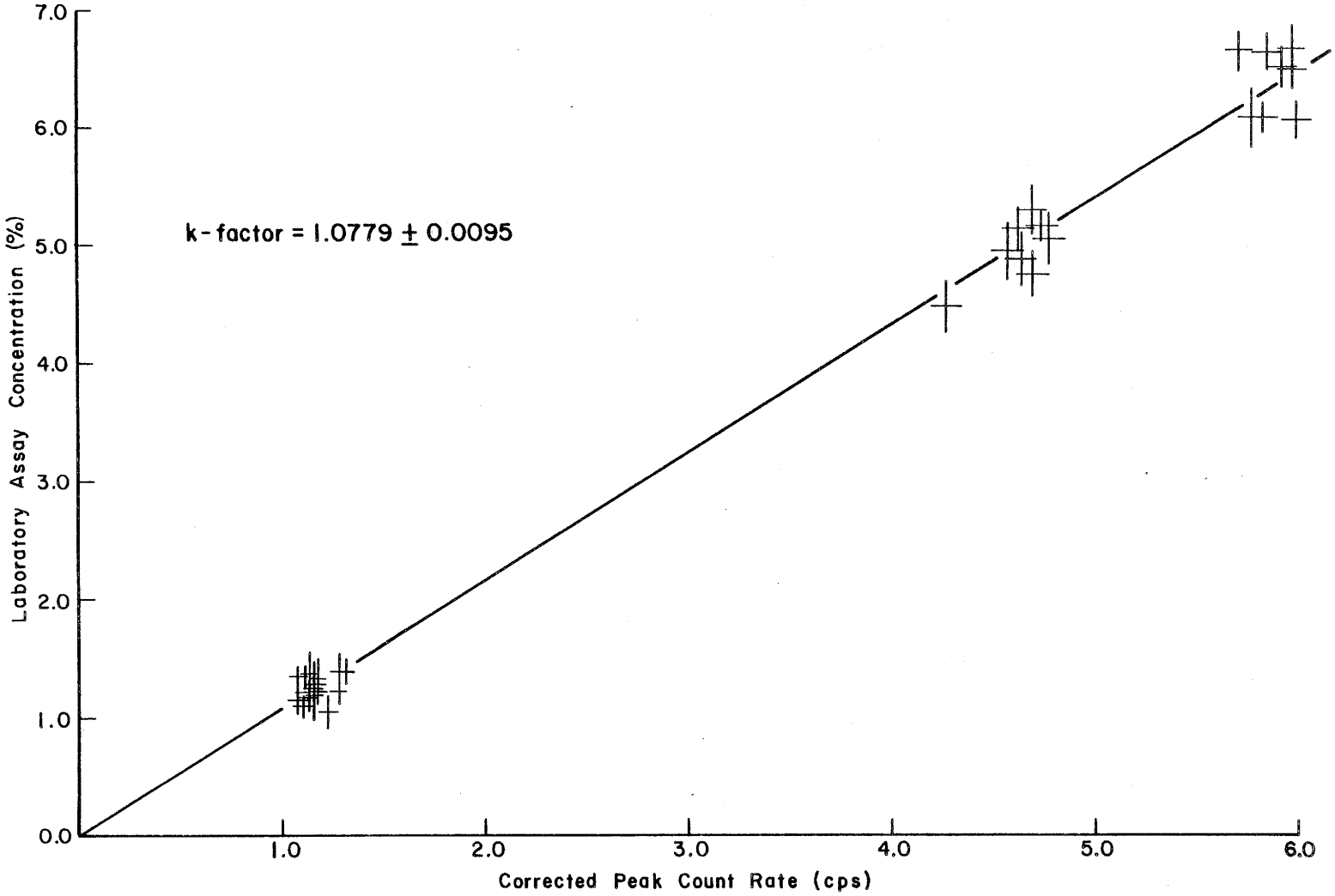

Figure 5-1. Potassium Data Regression

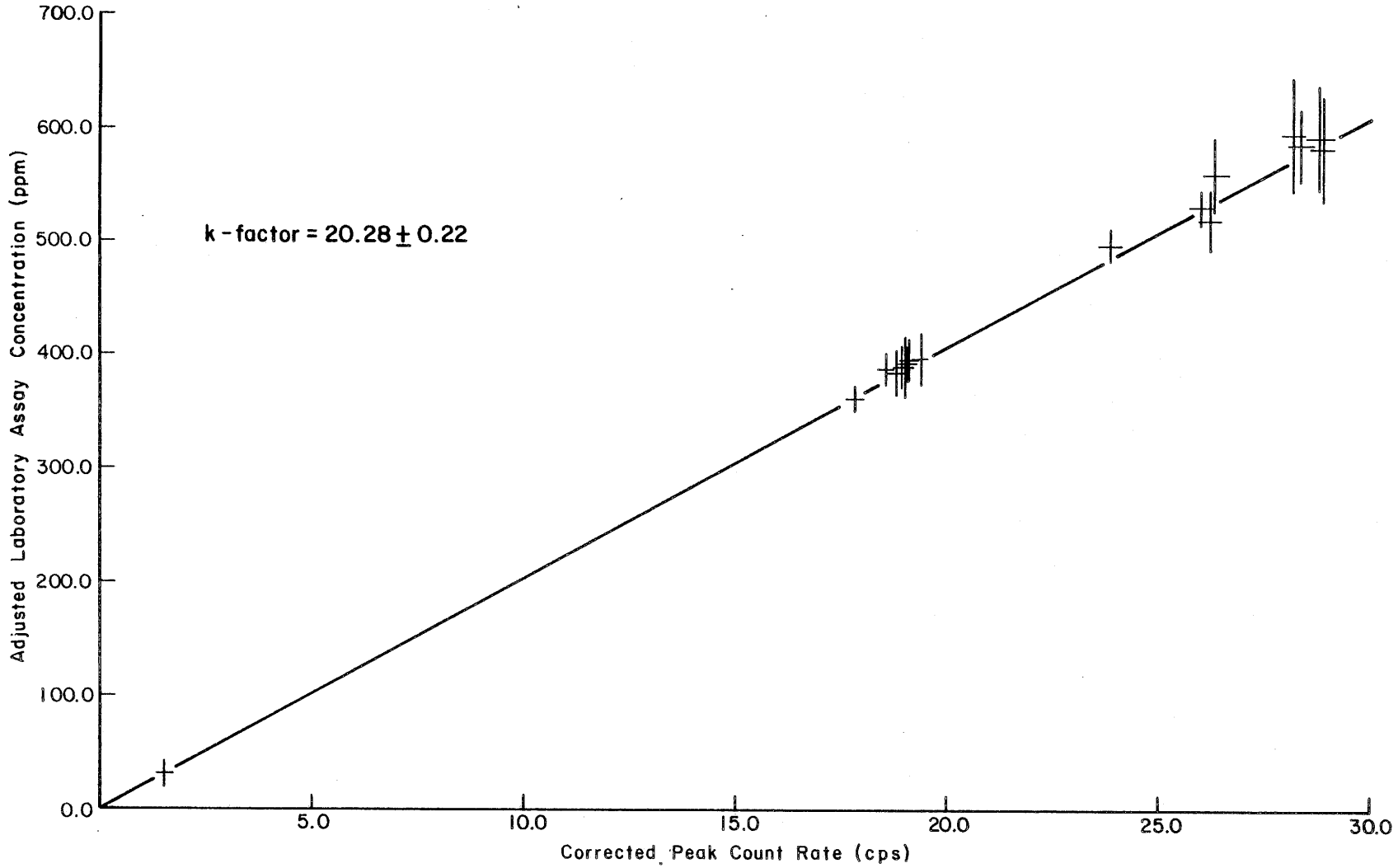

Figure 5-2. Uranium Data Regression (laboratory assay concentrations adjusted for Ra-226/U-238 disequilibrium in NBL standard)

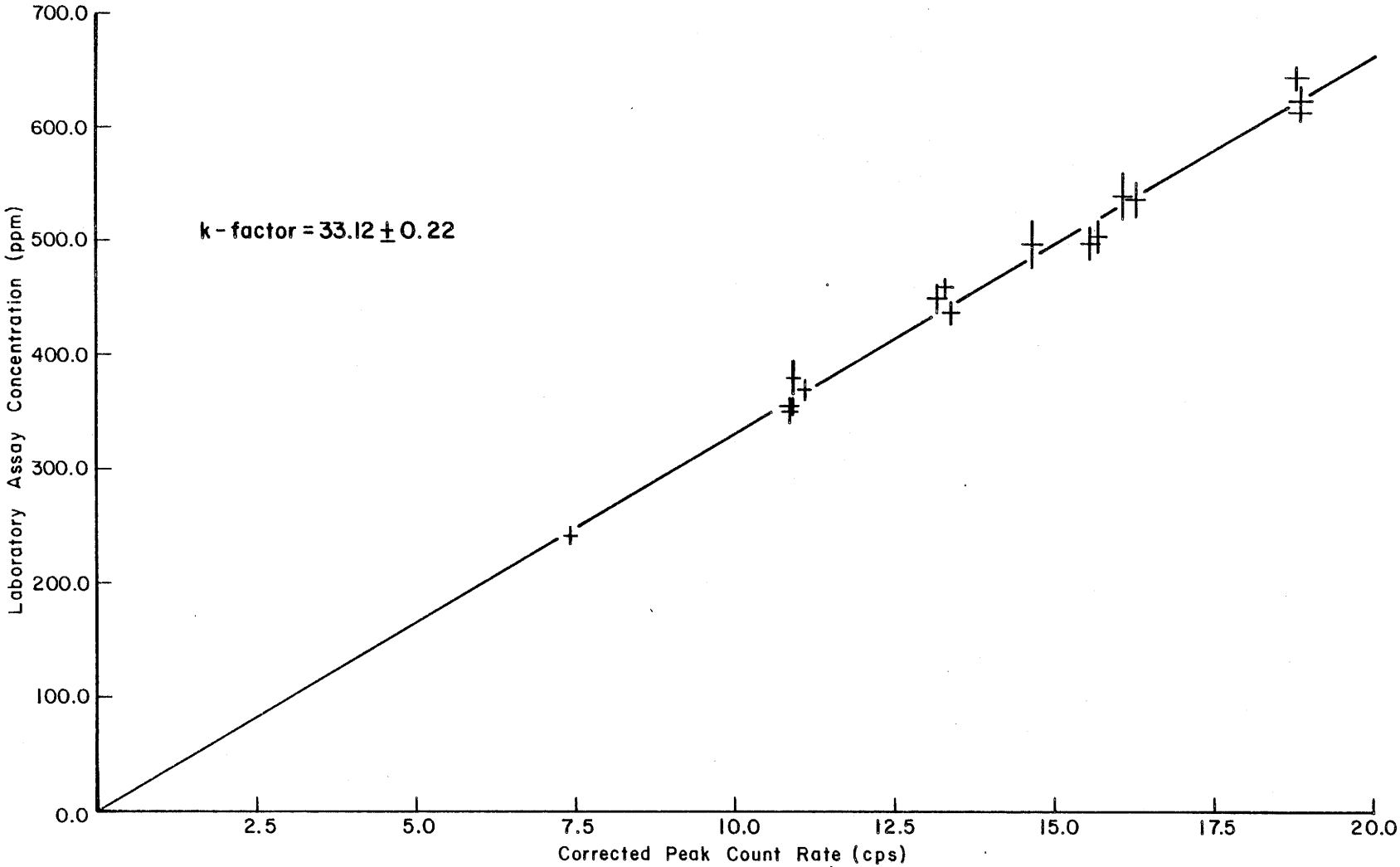

Figure 5-3. Thorium Data Regression

Figure 5-4 is a plot of the k-factors obtained for each model in the total-count study ($k_i = C_i/R_i$, where C_i is the laboratory assay concentration and R_i is the corrected in-situ count rate for the ith model) versus assay concentration. It is apparent from the plot that the eight U models as a subset have a larger average k-factor than that of the entire set of 39 models (0.06557±0.00152 ppm U/cps versus 0.06289±0.00042 ppm U/cps). It is also apparent that the six models containing the largest uranium concentrations in the total-count study have k-factors which are consistently below the average value, possibly as a result of inaccuracies in the corrections calculated for dead time and/or Z-effect, or in the correlation between the two gamma-ray detectors (probes) used in that previous work.

If the average k-factor of the U model subset is used with the corrected in-situ total-count data obtained in that study to calculate concentrations, the results agree statistically in every case with those determined in the present study (Table 5-3). Exclusion of the six data points for the largest uranium concentrations in the total-count study results in an average k-factor for the remaining 33-point data set of 0.06327±0.00050 ppm U/cps, which is still significantly less than that of the U model subset. However, if in addition to excluding these six models, the assay concentrations of the BA, SBA, MBA, RBA, GBA, CBA, TBA, and A1 models (the lowest-concentration models in the total-count study) are adjusted for the contributions of K-40 and Th-232 to their in-situ total count rates,* then the average total-count k-factor for the remaining 33-model set becomes 0.06359±0.00050 ppm U/cps. This value makes the U model subset appear considerably less anomalous.

*One percent potassium and 1 ppm thorium yield total count rates corresponding to apparent uranium concentrations of 1.5 and 0.4 ppm, respectively (George and Knight, 1982; George and Price, 1982).

Table 5-3. Comparison of Assigned Uranium Concentrations with Total-Count Assignments*

	Assigned Uranium Concentration (ppm)**		
Model	Total-Count Study	Total-Count Study, 'U' Subset Only	Present Study
U	472.5 ± 8.2	492.4 ± 13.9	488.2 ± 8.0
BU	557.1 ± 9.1	580.7 ± 16.0	583.2 ± 8.9
CBU	506.4 ± 8.3	527.9 ± 14.6	527.3 ± 8.4
TBU	504.8 ± 8.3	526.1 ± 14.6	530.5 ± 8.3
GBU	501.4 ± 8.1	522.6 ± 14.4	534.0 ± 8.2
MBU	547.2 ± 8.8	570.3 ± 15.7	584.6 ± 8.9
RBU	561.4 ± 9.1	585.1 ± 16.1	574.7 ± 8.8
SBU	555.9 ± 9.1	579.4 ± 16.0	571.0 ± 8.7

*Total-count assignments from George and others, 1983.

**Uncertainties are one standard deviation (68 percent confidence interval).

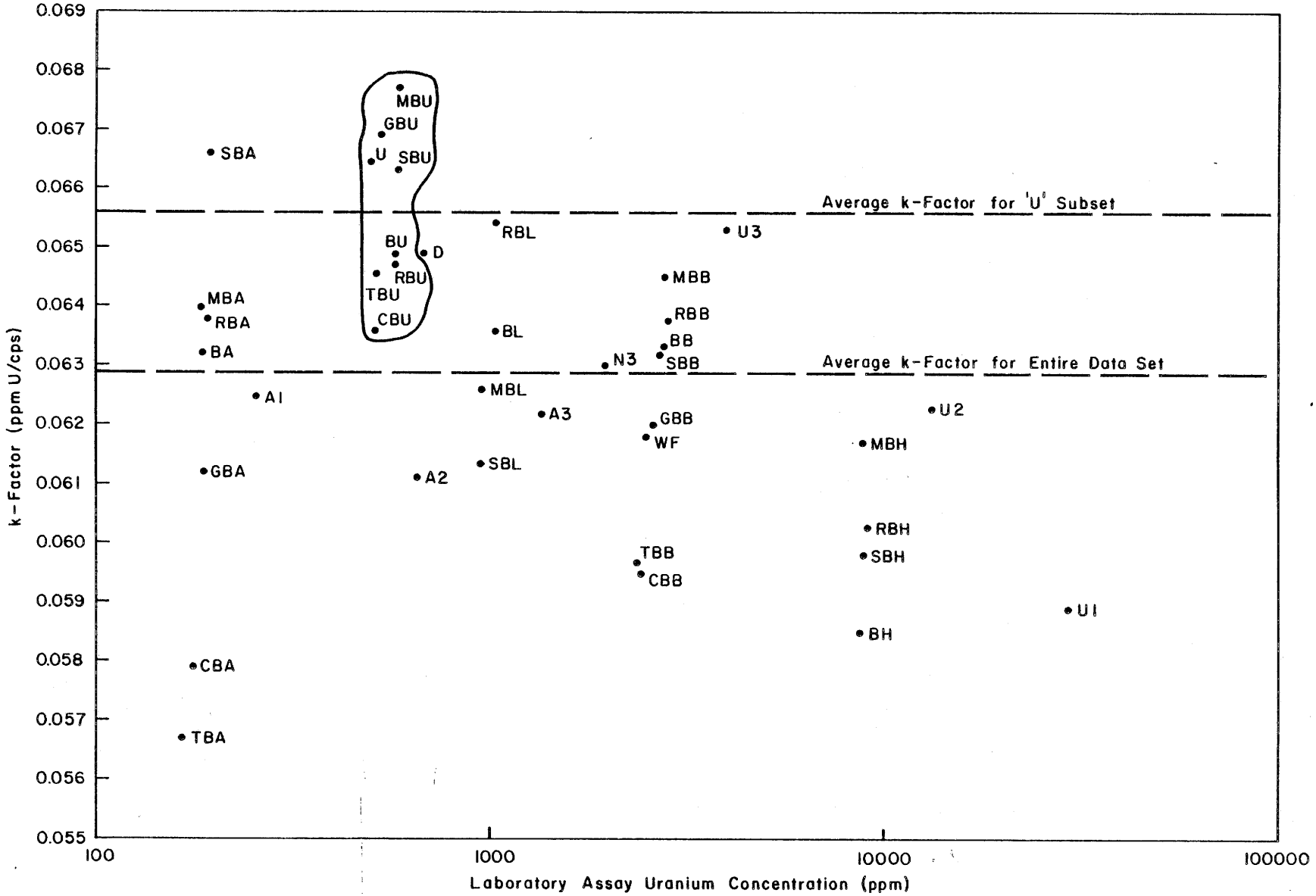

Figure 5-4. Total-Count k-Factors Versus Laboratory Assay Concentrations

It is still possible that sampling errors produced higher laboratory assay values for the U models, or that significantly different concrete matrices in these models result in lower in-situ count rates than would be expected for their actual uranium concentrations. Whatever the cause, we do not presently have sufficient information to reliably explain the source of these discrepancies, nor to choose one set of values as being definitely preferable to the other. On the other hand, since the magnitudes of the discrepancies are relatively small, the use of one set of values instead of the other in an actual instrument calibration would probably make little difference in the resulting uranium k-factor. The discrepancies could then be translated into slightly larger uncertainties in the uranium concentrations inferred from field measurements made with the instrument.

6.0 COMPARISON WITH SODIUM IODIDE DETECTOR DATA

The self-consistency of the concentrations assigned to the spectral gamma-ray borehole models was checked using data acquired with a sodium iodide (NaI) detector associated with the Calibration Facilities Monitoring System. The detector was calibrated at each of the field sites (with the exception of Morgantown, cf. Section 3.2), at the Grand Junction B-models, and at the Grand Junction KUT models (including the KW model).

The data were acquired in the center of the enriched zone of each model (see Appendix D, Sodium Iodide Data from the Mid-Enriched Zone). A series of spectra were collected at the same point, primarily to enable the software stabilization routine to calculate the adjusted energy to channel-number calibration coefficients, but also to provide a means for determining the repeatability of the measurements.

The raw data were corrected for dead-time effects using an equation derived from a multiple regression on a set of two-source measurements (George and others, 1983). This correction has the form

$$W_c = W_o(1 + d_0T_o + d_1T_o^2 + d_2T_o^3 + d_3T_o^4)$$

where W_c is the dead-time-corrected window count rate (either K, U, or Th), W_o is the observed window count rate, T_o is the observed total count rate, and d_0, d_1, d_2, and d_3 are the coefficients determined for the dead-time correction from the two-source measurements.

These count rates were also corrected for moisture effects. The same basic correction procedure that was used for the HPGe data was used for the NaI data, in that the moisture correction factor is based on the ratio of the linear attenuation coefficients for the wet and dry concrete of a model. Although the windows of the NaI spectra do not correspond to a single energy as well as the peaks in the HPGe spectra do, it was assumed that the average energy of the spectral window could be used. This assumption is valid because, although the linear attenuation coefficients for water and concrete change significantly with energy, the ratio of the two coefficients remains relatively constant. For the potassium and thorium windows, this average energy is the energy of the peaks used in the HPGe spectra, and thus the corrections have the same values as those determined previously (cf. Section

4.1.2). The uranium window has been set up to include both the 1765-keV peak and the 2204-keV peak. The moisture correction factor used for this case was the average of the corrections for these two energies, weighted by the relative intensities of the two gamma rays.

The corrected count rates used in these calibrations are listed in Table 6-1. The uncertainties assigned to these count rates are based on the observed variation of the window count rates measured in each spectrum about the average for the window and the model. The contributions from the uncertainties in the correction factors were assumed to be constant, 1.03 percent for the moisture correction factor and 0.10 percent for the dead-time correction factor.

Table 6-1. Corrected Count-Rate Data from CFMS NaI Detector

Model	Potassium Window* (cps)	Uranium Window* (cps)	Thorium Window* (cps)
K	4.01 ± 0.06	0.44 ± 0.01	0.05 ± 0.004
U	49.95 ± 0.84	41.80 ± 0.70	0.54 ± 0.06
T	20.11 ± 0.32	31.45 ± 0.83	7.34 ± 1.05
KW	45.29 ± 0.53	45.82 ± 0.80	4.76 ± 0.16
BK	4.18 ± 0.06	0.37 ± 0.01	0.03 ± 0.003
BU	57.52 ± 0.71	48.59 ± 0.73	0.81 ± 0.05
BT	22.63 ± 0.31	36.01 ± 0.50	9.03 ± 0.18
BM	53.41 ± 0.75	56.81 ± 0.92	6.77 ± 0.12
CBK	4.16 ± 0.09	0.39 ± 0.03	0.02 ± 0.01
CBU	52.73 ± 0.82	44.50 ± 0.64	0.67 ± 0.06
CBT	25.18 ± 0.43	48.14 ± 0.65	10.67 ± 0.26
CBM	54.03 ± 0.66	60.49 ± 0.91	8.37 ± 0.26
TBK	4.05 ± 0.17	0.36 ± 0.02	0.03 ± 0.02
TBU	51.87 ± 0.86	44.09 ± 0.75	0.71 ± 0.02
TBT	23.85 ± 0.52	46.15 ± 0.64	10.77 ± 0.17
TBM	55.29 ± 0.73	61.47 ± 0.75	7.70 ± 0.13
GBK	4.05 ± 0.12	0.38 ± 0.03	0.03 ± 0.01
GBU	52.74 ± 0.70	44.95 ± 0.61	0.79 ± 0.07
GBT	25.35 ± 0.33	42.76 ± 0.60	10.37 ± 0.18
GBM	55.51 ± 0.80	63.10 ± 0.77	7.96 ± 0.31
RBK	4.21 ± 0.10	0.42 ± 0.01	0.04 ± 0.004
RBU	55.92 ± 0.78	47.98 ± 0.60	1.22 ± 0.09
RBT	21.55 ± 0.34	35.14 ± 0.41	8.67 ± 0.12
RBM	48.97 ± 0.65	51.86 ± 0.78	6.40 ± 0.16
SBK	4.30 ± 0.10	0.41 ± 0.03	0.02 ± 0.01
SBU	56.96 ± 0.70	48.68 ± 0.62	0.95 ± 0.06
SBT	22.06 ± 0.28	42.02 ± 0.57	9.35 ± 0.21
SBM	52.18 ± 0.65	56.96 ± 0.75	6.55 ± 0.12

*Uncertainties cited are 1 standard deviation (68 percent confidence interval).

The calibration coefficients for the NaI detector were determined from a multiple linear regression of corrected window count rates versus assigned concentrations. The equations used for the regression are

$$K\ (\%) = a_{11}W_K + a_{12}W_U + a_{13}W_T$$

$$U\ (ppm) = a_{22}W_U + a_{23}W_T$$

$$Th\ (ppm) = a_{32}W_U + a_{33}W_T$$

where K, U, and Th are the concentrations for potassium, uranium, and thorium; W_K, W_U, and W_T are the window count rates for potassium, uranium, and thorium corrected for dead time and moisture; and a_{11}, a_{12}, a_{13}, a_{22}, a_{23}, a_{32}, and a_{33} are the calibration coefficients to be determined. These coefficients (Table 6-2) were determined for each set of models, as well as for the total model set (i.e., all models in which data were acquired).

Also listed in Table 6-2 are the data used to compare these calibration coefficient sets. The measured uncertainty is determined from the variance of the indicated coefficients about the average value for that coefficient. The estimated uncertainty is determined from the uncertainties in the corrected NaI detector count rates and the uncertainties in the assigned concentrations. In other words, the estimated uncertainty is the fluctuation we expected to see in the data, and the measured uncertainty is the fluctuation we did see. The F-statistic is the appropriate test to use in comparing these two uncertainties. All of the calculated values lie within the 98 percent confidence limits; however, one value (for coefficient a_{23}) does lie outside the 90 percent confidence limits, indicating that we observed more variance in the value of this coefficient than we could predict from the data.

Table 6-2. Calibration Coefficients Determined for the CFMS NaI Detector

	Potassium			Uranium		Thorium	
Parameter	a_{11}	a_{12}	a_{13}	a_{22}	a_{23}	a_{32}	a_{33}
Grand Junction							
KUT Models	0.499	0.0990	0.0339	0.0852	0.0606	0.00151	0.0155
B Models	0.572	0.0967	0.0347	0.0836	0.0630	0.00131	0.0168
Casper	0.562	0.0974	0.0331	0.0814	0.0706	0.00142	0.0173
George West	0.617	0.0964	0.0326	0.0814	0.0692	0.00084	0.0171
Grants	0.593	0.0968	0.0343	0.0850	0.0654	0.00137	0.0166
Reno	0.483	0.0943	0.0332	0.0812	0.0617	0.00170	0.0165
Spokane	0.607	0.0979	0.0344	0.0836	0.0733	0.00132	0.0173
All Models	0.564	0.0969	0.0337	0.0830	0.0668	0.00136	0.0168
Uncertainty							
Measured	9.2%	2.9%	2.3%	2.1%	7.3%	19.5%	3.8%
Estimated	9.9%	1.8%	2.6%	1.9%	2.5%	24.1%	8.8%
F-Statistic*	0.86	2.60	0.78	1.22	8.53	0.66	0.19

*The 98 percent confidence region is 0.08 through 12.25; the 90 percent confidence region is 0.18 through 5.59.

7.0 STABILITY

The stability of the instruments used to make the measurements in the models affects the accuracy with which the measurements can be made. The stability of the HPGe detector was monitored by periodically measuring the 1765-keV peak count rate from a Ra-226 standard 'button' source in a repeatable geometry and by measuring the full-width-at-half-maximum (FWHM) amplitude of the same peak. These measurements indicate that the variation from measurement to measurement can be explained by counting statistics alone, or that the instrument itself has a fluctuation in gain or resolution of less than 1 percent. Table 7-1 presents the data for this series of stability measurements; Figure 7-1 portrays the data graphically.

Stability measurements for the neutron probe were taken with the source in its fixed position in its carrying 'pig.' As noted in Section 3.1, the data indicate a distinct change in the epithermal neutron count rate between the time when the truck left the George West site and the time at which pretrip measurements were made for the Reno, Spokane, and Casper visits. This observed change was attributed to an increase in background noise in the detector. A power supply was subsequently replaced; this reduced the noise, but not to its original level. To avoid observing this noise as signal, the threshold for the epithermal region of the spectrum was increased. This resulted in a slight decrease in the observed epithermal neutron count rate, from an average of 88.88 cps before the change to an average of 86.21 cps after the change. The ratio of these sensitivity values was applied as a correction factor to the epithermal neutron count rates measured in the models at Reno, Spokane, and Casper; these data are presented in Table 7-2 and Figure 7-2.

Stability data for the NaI detector were also acquired in the form of the total count rate measured from a radium standard source and the FWHM of the 661-keV peak from a Cs-137 standard source. These stability data for the NaI detector are presented in Table 7-3 and Figure 7-3.

Table 7-1. HPGe Detector Radium Efficiency Measurements

Sequence Number	Date Measured	1765-keV Peak Net Counts*	1765-keV Peak Resolution
1	4/28/83	1644.5 ± 42.0	2.38
2	4/28/83	1684.3 ± 43.1	2.47
3	4/28/83	1617.6 ± 41.6	2.43
4	4/28/83	1567.8 ± 41.1	2.59
5	4/28/83	1575.4 ± 41.5	2.34
6	6/03/83	1593.1 ± 41.6	2.35
7	6/03/83	1715.1 ± 43.2	2.47
8	6/08/83	1617.6 ± 41.9	2.52
9	6/08/83	1559.1 ± 41.2	2.52
10	6/08/83	1706.7 ± 42.5	2.45
11	6/08/83	1671.0 ± 42.6	2.47
12	6/08/83	1663.6 ± 42.5	2.47
13	6/16/83	1616.7 ± 42.1	2.39
14	6/16/83	1638.7 ± 41.8	2.18
15	6/16/83	1602.3 ± 41.7	2.45
16	7/01/83	1690.8 ± 42.4	2.41
17	7/01/83	1674.8 ± 42.5	2.13
18	8/08/83	1614.8 ± 41.8	2.43
19	8/08/83	1709.4 ± 43.1	2.34
20	8/09/83	1603.2 ± 41.7	2.33
21	8/09/83	1714.5 ± 42.6	2.24
22	8/09/83	1552.9 ± 41.3	2.62
23	8/09/83	1611.9 ± 41.7	2.41
24	8/18/83	1612.4 ± 41.9	2.15
25	8/18/83	1611.7 ± 41.7	2.37
26	8/28/83	1550.9 ± 41.4	2.48
27	8/28/83	1560.7 ± 41.3	2.31
28	8/28/83	1560.7 ± 40.9	2.44
29	8/28/83	1529.6 ± 40.5	2.26
30	8/29/83	1568.3 ± 41.0	2.32
31	8/29/83	1569.4 ± 40.9	2.31
32	9/01/83	1571.8 ± 41.1	2.38
33	9/01/83	1641.2 ± 42.2	2.30
34	9/01/83	1559.2 ± 41.2	2.33
35	9/10/83	1665.8 ± 42.4	2.18
36	9/10/83	1556.7 ± 41.2	2.52
37	9/10/83	1597.1 ± 41.8	2.19
38	9/10/83	1621.0 ± 42.1	2.29
39	9/10/83	1634.9 ± 41.9	2.46
40	9/19/83	1634.3 ± 42.1	2.16
41	9/19/83	1582.7 ± 40.9	2.60

*Uncertainties cited are 1 standard deviation (68 percent confidence interval).

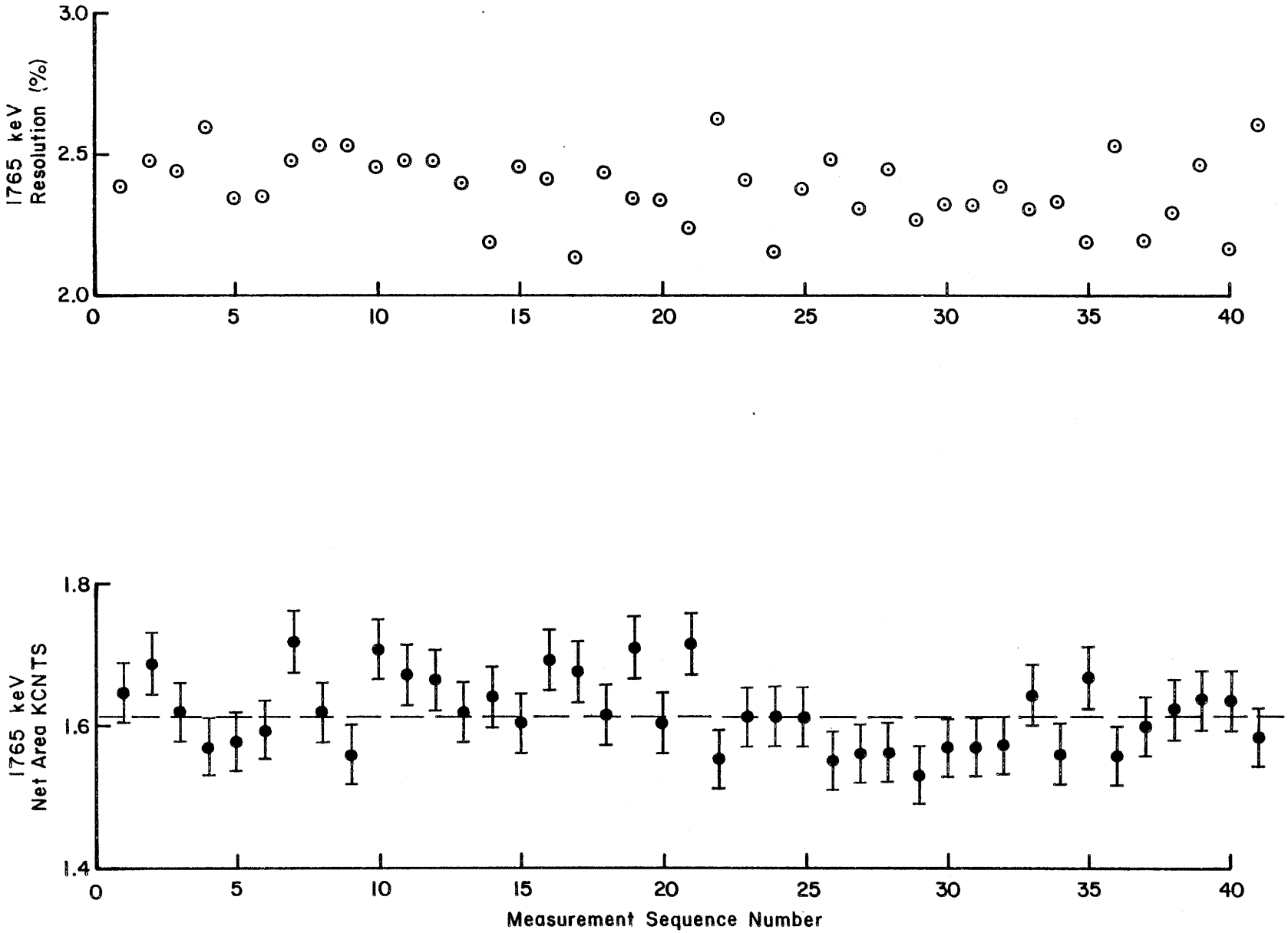

Figure 7-1. HPGe Detector System Stability

Table 7-2. Neutron-Neutron Probe Stability Measurements

Sequence Number	Date Measured	Total Count Rate (cps)	Epithermal Count Rate (cps)
1	4/08/83	102.4	86.7
2	4/08/83	104.0	88.5
3	4/08/83	105.6	88.1
4	4/20/83	103.1	88.0
5	4/21/83	105.5	88.8
6	6/01/83	101.8	89.1
7	6/01/83	104.2	89.8
8	6/09/83	109.5	88.6
9	6/09/83	107.3	88.1
10	6/09/83	105.5	88.5
11	6/15/83	105.6	88.9
12	6/16/83	102.2	89.3
13	6/17/83	101.3	88.8
14	6/17/83	106.6	90.1
15	6/17/83	105.9	90.0
16	6/17/83	103.7	90.7
17	8/24/83	98.5	85.1
18	8/24/83	98.1	85.7
19	8/24/83	98.3	86.9
20	8/28/83	99.7	86.8
21	8/28/83	98.2	86.9
22	9/07/83	100.6	84.9
23	9/07/83	102.1	86.4
24	9/07/83	100.1	85.5
25	9/12/83	107.6	86.1
26	9/12/83	102.1	87.6
27	9/12/83	101.0	86.4

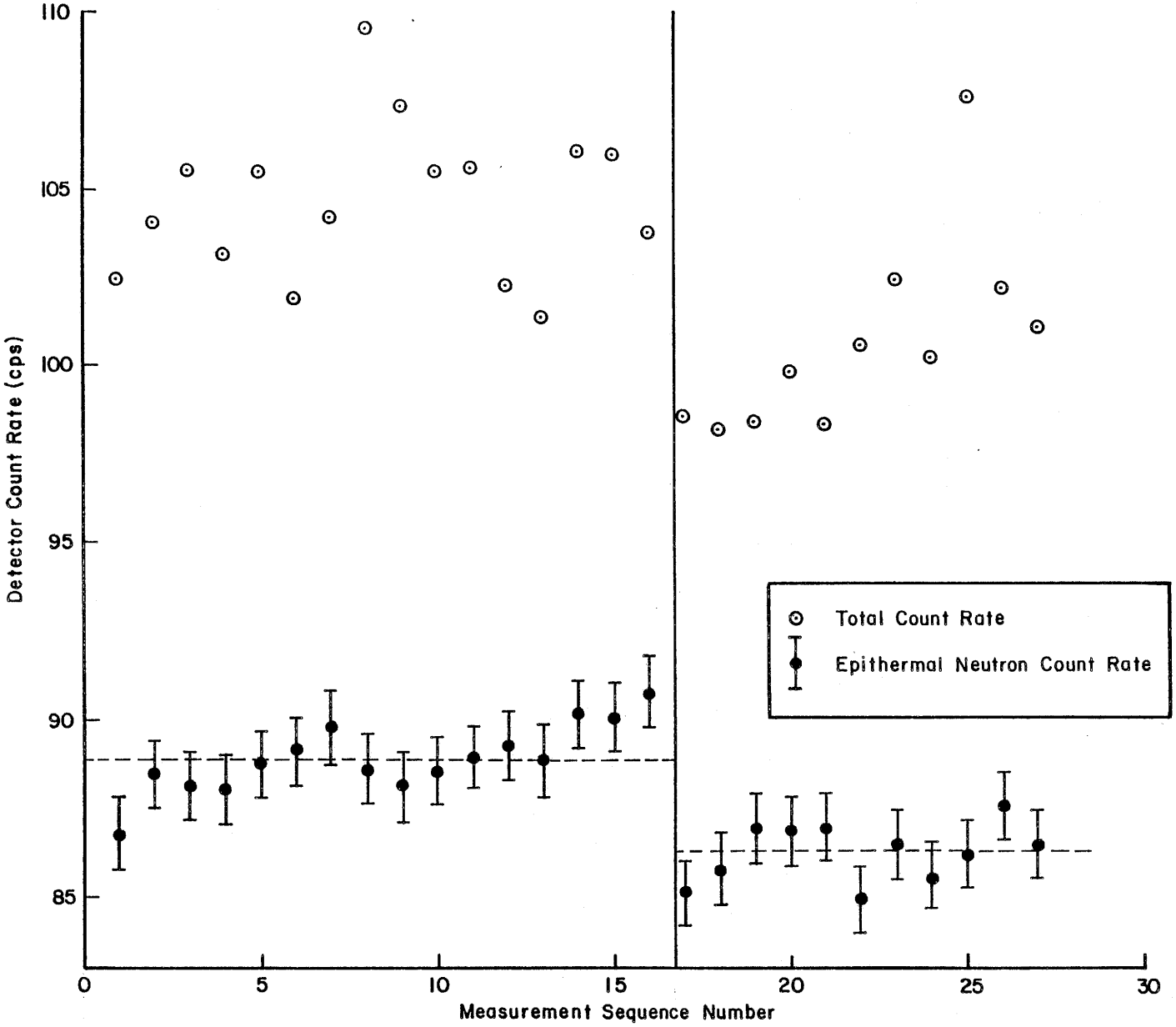

Figure 7-2. Neutron Probe Stability

Table 7-3. NaI Detector Stability Measurements

Sequence Number	Date Measured	Ra-226 Total Count Rate (cps)	Cs-137 661-keV Peak FWHM (%)
1	4/04/83	19741	7.89
2	4/05/83	19767	7.95
3	4/06/83	19614	7.81
4	4/07/83	19792	7.78
5	4/12/83	19899	7.87
6	5/13/83	19838	7.79
7	5/17/83	19776	8.02
8	6/03/83	19788	8.23
9	6/08/83	20057	7.90
10	6/08/83	20099	8.06
11	6/09/83	19875	7.86
12	6/14/83	20116	8.17
13	8/23/83	19598	---*
14	8/27/83	20212	8.22
15	8/28/83	20173	8.00
16	9/06/83	19992	8.12
17	9/07/83	19871	7.86
18	9/11/83	19984	8.01
19	9/12/83	20020	7.89
20	10/24/83	19949	7.72
21	10/25/83	19974	8.01

*The operator neglected to record the information necessary to calculate the full-width-at-half-maximum of the Cs-137 peak at 661 keV.

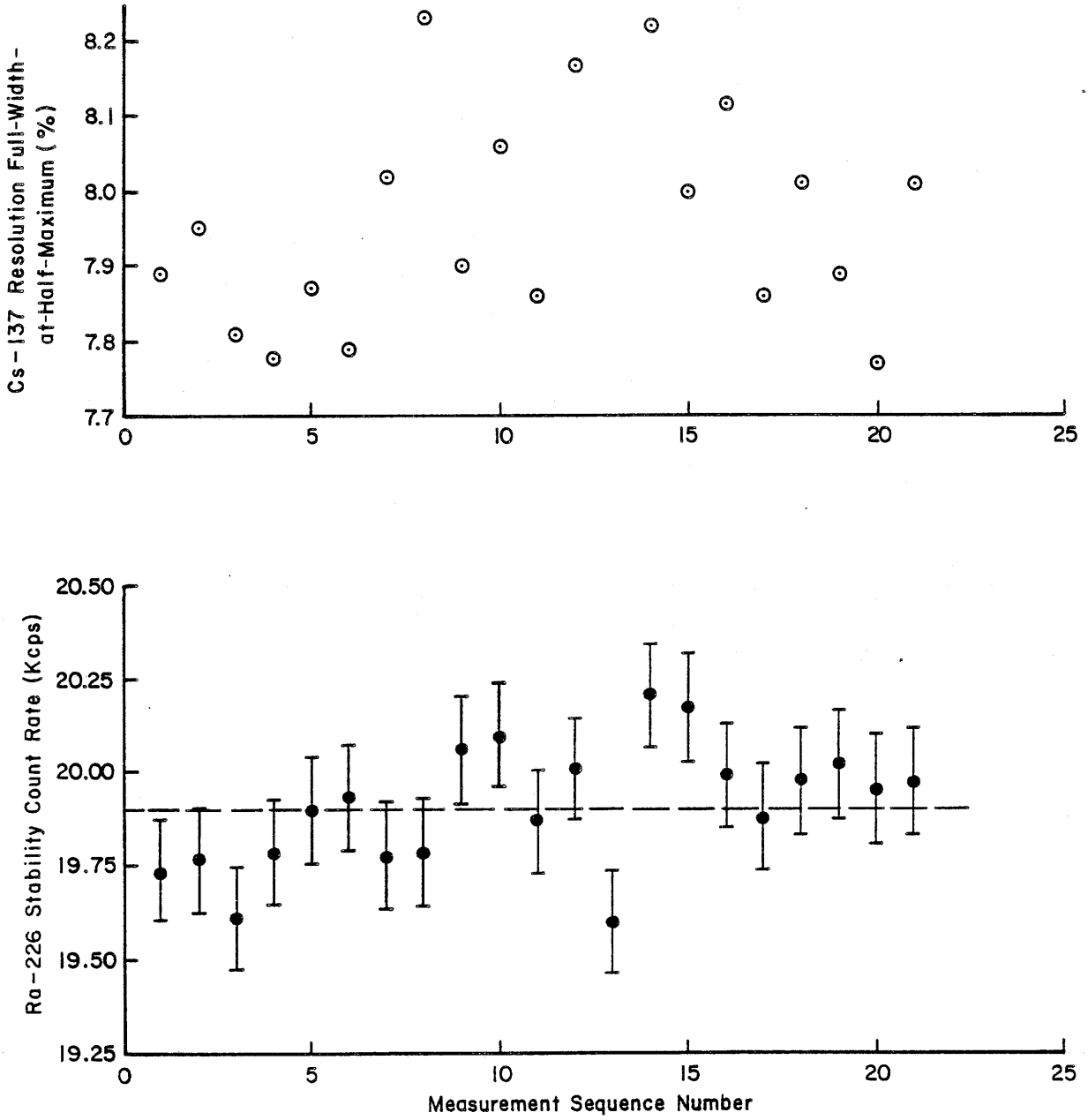

Figure 7-3. NaI Detector Stability

8.0 CONCLUSIONS AND RECOMMENDATIONS

The work documented in this report was performed to determine potassium, uranium, and thorium concentration assignments for the spectral gamma-ray borehole calibration models located at various sites across the country. The assignments were to be characterized by traceability to NBL standards and by self-consistency.

The former requirement was met through the use of assays performed by the Geochemistry Laboratory. Since the laboratory calibrated its radiometric assay detector using the NBL standards, it follows that the assay concentrations, and in turn the assigned concentrations, are based upon the values of these standards. Since few of the concentrations assigned to the models varied significantly from the assay values measured from the concrete samples, we feel that this traceability requirement has been met.

The latter requirement, that the concentrations be self-consistent, was addressed by using logging data to ensure consistency between the models. We expected that some potential problems, associated either with sampling errors in the determination of assay concentrations or with inhomogeneity within a model, might produce some discrepancy between the laboratory and the borehole measurements. We felt justified in our expectations when some of the assigned concentrations, albeit few, did vary significantly from the assay values.

Calibration coefficients for the sodium iodide detector, calculated using the data from different field sites, vary by only a few percent in most cases, and, in the majority of those cases, the observed variance could be predicted from the uncertainties in the measured count rates and in the assigned concentrations. The one exception, coefficient a_{23} (cf. Section 6.0), is most likely due to a larger-than-expected variance in the NaI detector data, since (1) the variance did not exceed the 98 percent confidence limits in the F-test (meaning that although it was a 1 in 20 occurrence, it was not a 1 in 100 occurrence), and (2) the problem did not arise in the regression of the HPGe data nor in the Geochemistry Laboratory data, both of which should have exhibited a similar problem if the assignment were incorrect.

The concentrations assigned to the models as a result of this study are accurate, consistent, and reliable. They represent a degree of accuracy greater than can be measured with the sodium iodide detectors currently in use. Because of the potential benefits accruing from the use of these models, we recommend that a measurement procedure be developed for calibration of spectral gamma-ray instruments based upon results of this study.

9.0 REFERENCES

Dechant, Gerald, 1984, Calibration and Performance of a High-Resolution Gamma Spectroscopy System: Grand Junction Area Office, U.S. Department of Energy Open-File Report, in preparation.

Duray, J. R., 1977, The Measurement of the Moisture Concentration of Selected Test Model Ore Zones: Grand Junction, Colorado, Bendix Field Engineering Corporation Internal Report BFEC-1977-3.

George, D. C., and Knight, L., 1982, Field Calibration Facilities for Environmental Measurement of Radium, Thorium, and Potassium: Grand Junction, Colorado, U.S. Department of Energy Technical Measurements Center Report GJ/TMC-01(82).

George, D. C., and Price, R. K., 1982, Abbreviated Total-Count Logging Procedures for Use in Remedial Action: Grand Junction, Colorado, U.S. Department of Energy Technical Measurements Center Report GJ/TMC-03(82).

George, D. C., Heistand, B. E., and Krabacher, J. E., 1983, Grade Assignments for Models Used for Calibration of Gross-Count Gamma-Ray Logging Systems: Grand Junction Area Office, U.S. Department of Energy Open-File Report GJBX-39(83).

George, D. C., Novak, E. F., and Price, R. K., 1984, Calibration-Pad Parameter Assignments for In-Situ Gamma-Ray Measurements of Radium, Thorium, and Potassium: Grand Junction Area Office, U.S. Department of Energy Technical Measurements Center Report, in preparation.

Knapp, K. E., and Bush, W. E., 1976, Construction of the KUT Test Pits: Grand Junction Area Office, U.S. Department of Energy Open-File Report GJBX-49(76).

Murri, R., Novak, E. F., and Ruzycki, C., 1983, Mobile Gamma Spectroscopy System Operation: Grand Junction, Colorado, Bendix Field Engineering Corporation Internal Report BFEC-1983-1.

Trahey, N. M., Voeks, A. M., and Soriano, M. D., 1982, Grand Junction/New Brunswick Laboratory Interlaboratory Measurement Program: Part I—Evaluation; Part II—Methods Manual: Argonne, Illinois, New Brunswick Laboratory, NBL-303.

U.S. Department of Health, Education, and Welfare, 1970, Radiological Health Handbook: Washington, D.C., pp. 137-139.

Wilson, R. D., 1981, Fundamentals of Gamma-Ray Logging: Paper presented at Gamma-Ray Logging Workshop, sponsored by Bendix Field Engineering Corporation and U.S. Department of Energy, February 1981.

Wilson, R. D., and Stromswold, D. C., 1981, Spectral Gamma-Ray Logging Studies: Grand Junction Area Office, U.S. Department of Energy Open-File Report GJBX-21(81), pp. 151-152.

York, Derek, 1966, Least-Squares Fitting of a Straight Line: Canadian Journal of Physics, v. 44, pp. 1079-1086.

Appendix A

LABORATORY ASSAY DATA

(microfiche in pocket, back inside cover)

CONTENTS OF APPENDIX

This appendix contains the laboratory assay data for samples collected from the concrete pour at the time of each model's construction. Samples were assayed for concentrations of potassium, uranium, and thorium. The computer-generated data listing for each model contains the following information:

- INPUT FILE NAME - Requisition Number and Model Identifier
- TICKET - Sample Ticket Number
- LABNO - Laboratory Sample Number
- WT/DEV% - Sample Weight (grams) and Deviation from the Mean (percent)
- K%/+-%/DEV% - Potassium Concentration (percent), One Standard Deviation (percent), and Deviation from the Mean (percent)
- U-PPM/+-%/DEV% - Uranium Concentration (ppm), One Standard Deviation (percent), and Deviation from the Mean (percent)
- T-PPM/+-%/DEV% - Thorium Concentration (ppm), One Standard Deviation (percent), and Deviation from the Mean (percent)
- TCU/+-%/DEV% - Uranium Derived from Total Counts, One Standard Deviation (percent), and Deviation from the Mean (percent)

A summary of the tabular data includes the number of samples analyzed, estimated mean, and estimated, expected, and unaccounted variances for each type of analysis performed.

KEY TO MICROFICHE

The layout of Appendix A, as it appears on the microfiche, is presented in the diagram below, with frame numbers added so that data for a given model can be more easily found. The frame numbers are then listed and identified by the model designation.

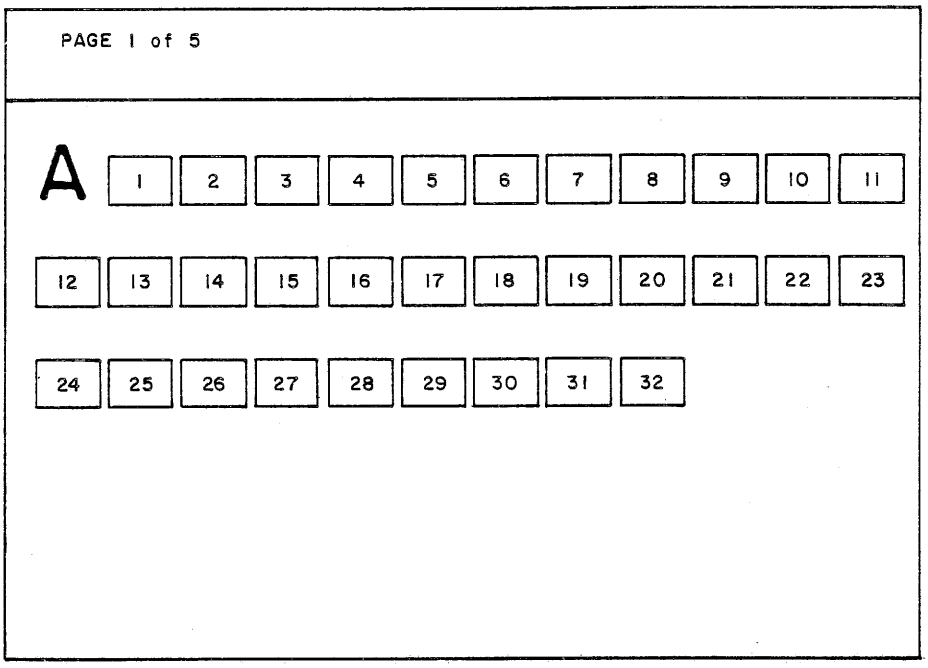

Frame No.	Model Designation	Frame No.	Model Designation
1	K	17	GBK
2	U	18	GBU
3	T	19	GBT
4	KW	20	GBM
5	BK	21	MBK
6	BU	22	MBU
7	BT	23	MBT
8	BM	24	MBM
9	CBK	25	RBK
10	CBU	26	RBU
11	CBT	27	RBT
12	CBM	28	RBM
13	TBK	29	SBK
14	TBU	30	SBU
15	TBT	31	SBT
16	TBM	32	SBM

Appendix B

NEUTRON PROFILES

(microfiche in pocket, back inside cover)

CONTENTS OF APPENDIX

The moisture in the models was measured using an epithermal neutron-neutron probe from the Calibration Facilities Monitoring System (CFMS). This appendix contains the resulting neutron profiles; a data listing and a profile plot are presented for each model measured. No data from the Morgantown site were collected with the neutron probe during this study because of difficulties encountered with the multichannel analyzer in the CFMS; however, profile plots for these models, acquired during a previous site visit, are included here.

Data Listings

The following information is presented at the top of each data listing. Items preceded by an H are program headers; those preceded by a C are operator comments.

- GSIZ - Number of Settings Active in the Multichannel Analyzer
- PHAL - Indicates Use of Live Time Clock for Acquisition Time
- AQUIRE TIME - Acquisition Time (seconds)
- PTOT - Preset Number of Counts on Which To Halt Acquisition (optional)
- *** K *** - Model Designation, in this case K
- 11.0' UP TO 1.3' @ 15 SEC/0.1' (example) - Depth Range Measured in Model at Live Time Acquisition per Depth Increment
- PREPIGTOT - Premeasurement Calibration Total Count Rate (cps) in Neutron Pig
- R Numbers - Premeasurement Calibration Epithermal Count Rates (cps) at Regions of Interest

In addition, pertinent remarks and/or questions with respect to any special conditions or problems are noted.

The columns of each data listing are identified as follows:

- Column 1 - D = Data
- Column 2 - Depth (feet)

- Column 3 - Clock Time (seconds)
- Column 4 - Not Used
- Column 5 - Epithermal Neutron Counts
- Column 6 - Not Used

Profile Plots

The following abbreviations are used in the legends of the profile plots:

- ROI - Region of Interest
- LT - Live Time
- INCR - Increment
- PRE PIG TOT CR or PIG TOTAL CR - Premeasurement Calibration Total Count Rate (cps) in Neutron Pig
- PIG EPITHERMAL CR - Premeasurement Calibration Epithermal Count Rates (cps) in Neutron Pig

KEY TO MICROFICHE

The layout of Appendix B, as it appears on the microfiche, is presented in the diagram below, with frame numbers added so that data for a given model can be more easily found. The frame numbers are then listed and identified by the model designation. Frames 1 through 56 contain the data listings; frames 57 through 88 are the profile plots. Note that the data listing for each model requires two consecutive frames.

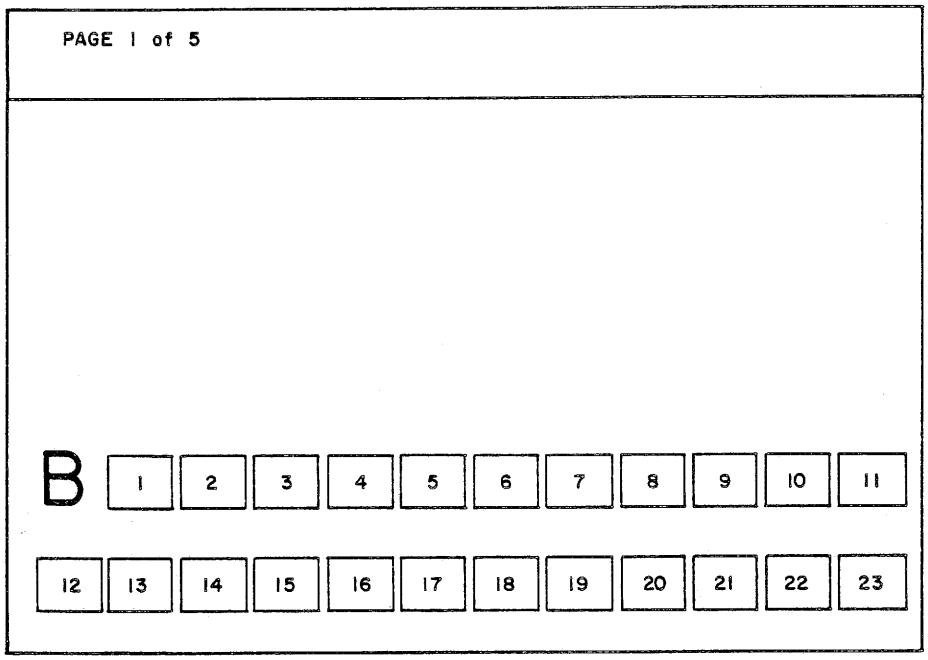
PAGE 1 of 5
B
1
2
3
4
5
6
7
8
9
10
11
12
13
14
15
16
17
18
19
20
21
22
23

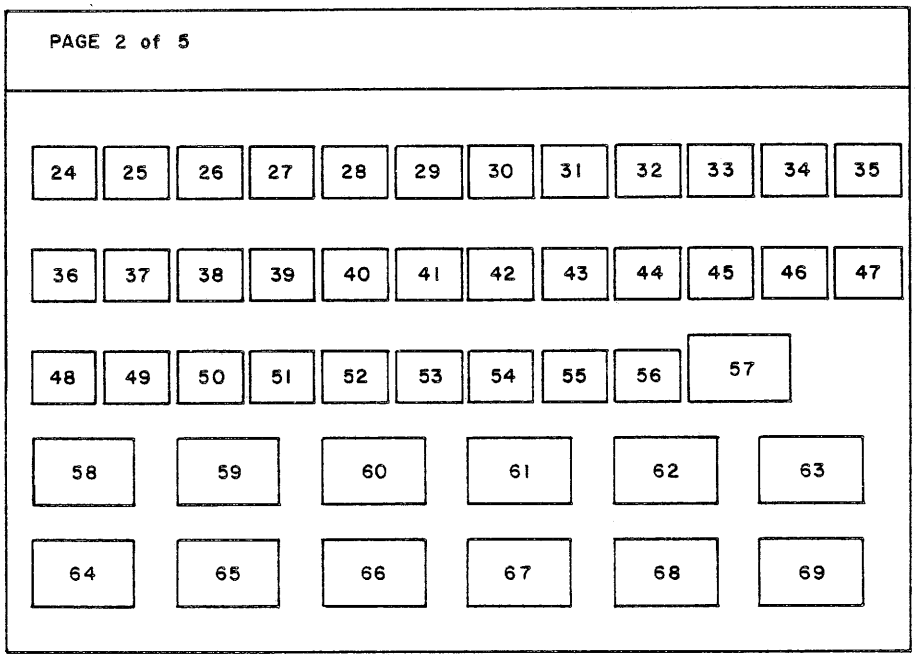
PAGE 2 of 5
24
25
26
27
28
29
30
31
32
33
34
35
36
37
38
39
40
41
42
43
44
45
46
47
48
49
50
51
52
53
54
55
56
57
58
59
60
61
62
63
64
65
66
67
68
69

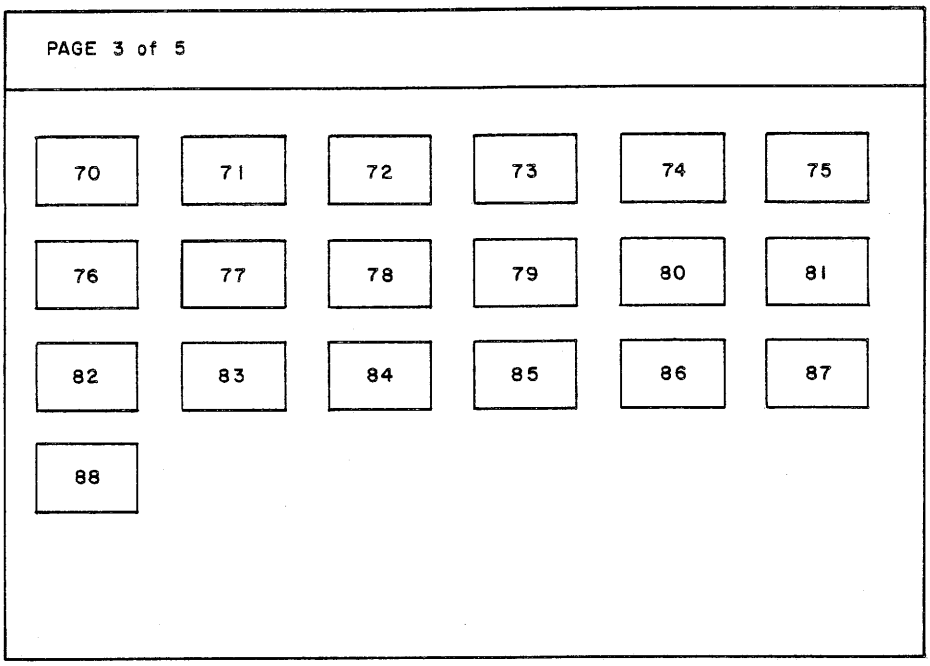

Frame No.	Model Designation	Frame No.	Model Designation
1-2	K	59	T
3-4	U	60	KW
5-6	T	61	BK
7-8	KW	62	BU
9-10	BK	63	BT
11-12	BU	64	BM
13-14	BT	65	CBK
15-16	BM	66	CBU
17-18	CBK	67	CBT
19-20	CBU	68	CBM
21-22	CBT	69	TBK
23-24	CBM	70	TBU
25-26	TBK	71	TBT
27-28	TBU	72	TBM
29-30	TBT	73	GBK
31-32	TBM	74	GBU
33-34	GBK	75	GBT
35-36	GBU	76	GBM
37-38	GBT	77	RBK
39-40	GBM	78	RBU
41-42	RBK	79	RBT
43-44	RBU	80	RBM
45-46	RBT	81	SBK
47-48	RBM	82	SBU
49-50	SBK	83	SBT
51-52	SBU	84	SBM
53-54	SBT	85	MBK
55-56	SBM	86	MBU
57	K	87	MBT
58	U	88	MBM

Appendix C

HIGH-PURITY GERMANIUM (HPGe) DETECTOR DATA FROM THE MID-ENRICHED ZONE

(microfiche in pocket, back inside cover)

CONTENTS OF APPENDIX

A high-purity germanium (HPGe) detector was used to acquire data from the enriched zones in the models (cf. Section 4.0 for detailed discussion of data acquisition and analysis). The following spectral-analysis data are presented in this appendix:

- GROSS COUNTS STEM TO STEARN - Total Counts in the Spectrum
- GROSS - Total Counts in the Photopeak
- NET/UNC - Net Counts in the Photopeak and One-Sigma Uncertainty
- T. BKG/UNC - Compton Background Counts and One-Sigma Uncertainty
- BLOW and BHIGH - Average Compton Background Counts in the Six Low and High Channels on Each Side of the Photopeak
- ICH-L and ICH-U - Lower and Upper Channel Numbers Delimiting the Photopeak
- DIF - Width of Photopeak Area (channels)
- FWHM - Full Width at Half Maximum of the Photopeak (channels)
- CHAN - Centroid of the Photopeak (channel number)

At the top of each data listing, a line designated 'LABEL' identifies the model, indicates whether the measurement was unshielded (US), and lists the Trigger N, or T Number, which is the number of counts output by the pulser as measured by the scaler. Above the LABEL line, live time (LT) and clock time (CT), both in seconds, are noted. In all the models, 4096 channels were used.

KEY TO MICROFICHE

The layout of Appendix C, as it appears on the microfiche, is presented in the diagram below, with frame numbers added so that data for a given model can be easily found. The frame numbers are then listed and identified by the model designation. Note that data for models U and GBT are presented in four frames instead of just two. The extra frames contain information detailing the pulser peak, which was not detected by the reduction program due to the excessive drift in the amplitude of the pulser output; thus, pulser peaks for these two models were calculated manually.

PAGE 3 of 5

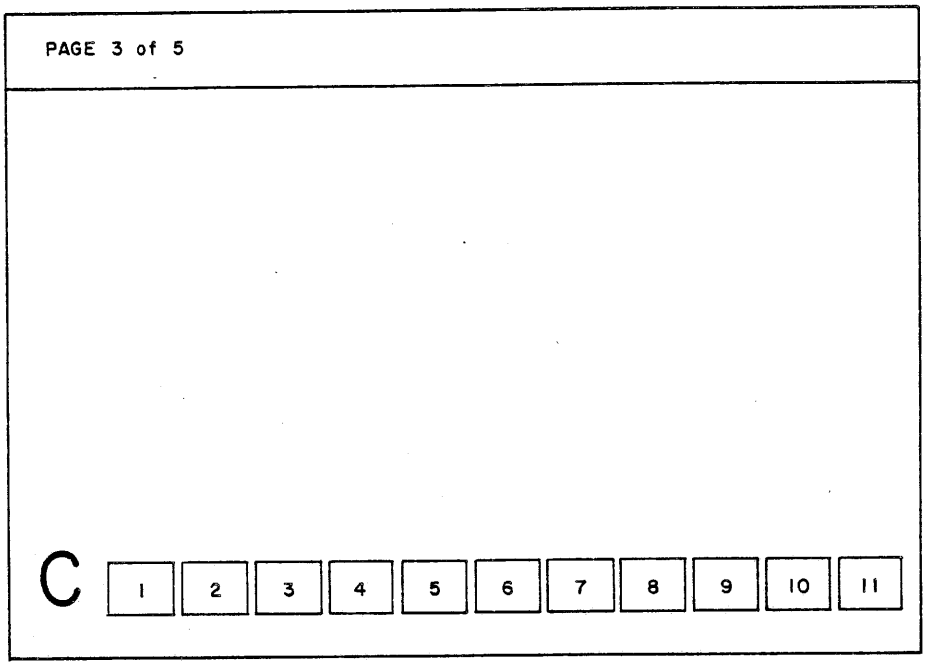

PAGE 4 of 5

12	13	14	15	16	17	18	19	20	21	22	23
24	25	26	27	28	29	30	31	32	33	34	35
36	37	38	39	40	41	42	43	44	45	46	47
48	49	50	51	52	53	54	55	56	57	58	59
60	61	62	63	64	65	66	67	68			

Frame No.	Model Designation	Frame No.	Model Designation
1-2	K	35-36	GBK
3-6	U	37-38	GBU
7-8	T	39-42	GBT
9-10	KW	43-44	GBM
11-12	BK	45-46	MBK
13-14	BU	47-48	MBU
15-16	BT	49-50	MBT
17-18	BM	51-52	MBM
19-20	CBK	53-54	RBK
21-22	CBU	55-56	RBU
23-24	CBT	57-58	RBT
25-26	CBM	59-60	RBM
27-28	TBK	61-62	SBK
29-30	TBU	63-64	SBU
31-32	TBT	65-66	SBT
33-34	TBM	67-68	SBM

Appendix D

SODIUM IODIDE DETECTOR DATA FROM THE MID-ENRICHED ZONE

(microfiche in pocket, back inside cover)

CONTENTS OF APPENDIX

A sodium iodide (NaI) detector, associated with the Calibration Facilities Monitoring System, was used to acquire data from the mid-enriched zone of each model; these data are presented in the listings contained in this appendix. No sodium iodide detector data were acquired at the Morgantown site because of difficulties encountered with the multichannel analyzer in the CFMS.

The following information is presented at the top of each data listing. Items preceded by an H are program headers; those preceded by a C are operator comments.

- GSIZ - Number of Settings Active in the Multichannel Analyzer
- PHAL - Indicates Use of Live Time Clock for Acquisition Time
- AQUIRE TIME - Acquisition Time (seconds)
- PTOT - Preset Number of Counts on Which To Halt Acquisition (optional)
- 15 x 3600 SEC. (example) - Number of Measurements and Acquisition Time of Each Measurement
- AO, 1, 2 - Calibration Coefficients for the Energy/Channel Number Relationship in the MCA
- RA SENS - Radium Sensitivity (cps)
- BG - Background Count Rate (cps)
- DEPTH - Depth Measured in Model
- **: K :** - Model Designation, in this case K

Any other information pertinent to data interpretation is also noted.

In the data listing, two lines are required to report the results of each measurement; hence, D identifies the first line of data and D& is the continuation line. The data presented for each measurement and the spaces they occupy on the data lines are as follows:

- Space 1 - Acquisition (Measurement) Number
- Space 2 - Clock Time (seconds)
- Spaces 3 and 4 - Total Counts, Gross and Net, respectively

- Spaces 5 and 6 - Potassium Counts, Gross and Net, respectively
- Spaces 7 and 8 - Uranium Counts, Gross and Net, respectively
- Spaces 9 and 10 - Thorium Counts, Gross and Net, respectively
- Spaces 11 and 12 - High-Energy Region of Interest (counts), Gross and Net, respectively

KEY TO MICROFICHE

The layout of Appendix D, as it appears on the microfiche, is presented in the diagram below, with frame numbers added so that data for a given model can be easily found. The frame numbers are then listed and identified by model designation. For each model, the first frame contains the raw data file; the second frame contains the data corrected for dead time.

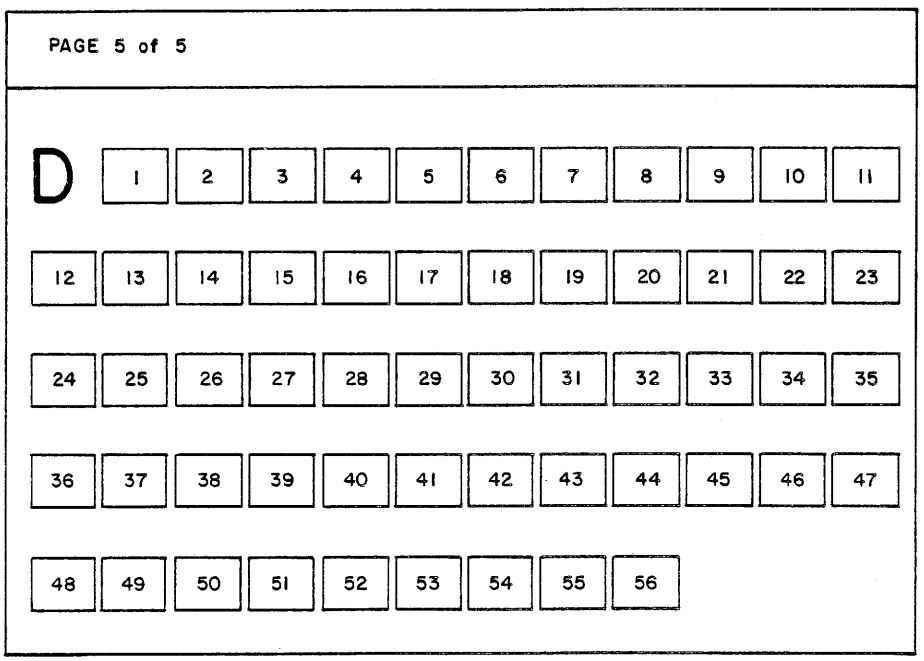

Frame No.	Model Designation	Frame No.	Model Designation
1-2	K	29-30	TBT
3-4	U	31-32	TBM
5-6	T	33-34	GBK
7-8	KW	35-36	GBU
9-10	BK	37-38	GBT
11-12	BU	39-40	GBM
13-14	BT	41-42	RBK
15-16	BM	43-44	RBU
17-18	CBK	45-46	RBT
19-20	CBU	47-48	RBM
21-22	CBT	49-50	SBK
23-24	CBM	51-52	SBU
25-26	TBK	53-54	SBT
27-28	TBU	55-56	SBM